

CHALMERS



Detection of Electrical Treeing in XLPE Exposed to AC and DC Stress

Diploma Work in the Master programme of Electric Power Engineering

ANETTE B. JOHANSSON
ANNA-MARIA B. SANDBERG

Department of Materials and Manufacturing Technology
Division of High Voltage Engineering
CHALMERS UNIVERSITY OF TECHNOLOGY
Gothenburg, Sweden, 2010
Diploma work No. 23/2010

Detection of Electrical Treeing in XLPE Exposed to AC and DC Stress

by

ANETTE B. JOHANSSON
ANNA-MARIA B. SANDBERG

Diploma work No. 23/2010

at the Department of Materials and Manufacturing Technology
CHALMERS UNIVERSITY OF TECHNOLOGY
Gothenburg, Sweden

Diploma work in the Master programme of Electric Power Engineering

Performed at: Chalmers University of Technology
SE-412 96 Gothenburg, Sweden

Supervisor: Dr. Björn Sonerud
Department of Materials and Manufacturing Technology
Chalmers University of Technology, SE-412 96 Gothenburg,
Sweden

Examiner: Prof. Stanislaw Gubanski
Department of Materials and Manufacturing Technology
Chalmers University of Technology, SE-412 96 Gothenburg,
Sweden

Detection of Electrical Treeing in XLPE Exposed to AC and DC Stress

ANETTE B. JOHANSSON
ANNA-MARIA B. SANDBERG

© ANETTE B. JOHANSSON & ANNA-MARIA B. SANDBERG, 2010.

Diploma work no 23/2010
Department of Materials and Manufacturing Technology
Chalmers University of Technology
SE-412 96 Gothenburg
Sweden
Telephone + 46 (0)31-772 1000

Cover: Electrical tree in XLPE initiated by DC voltage, page 45

Chalmers Reproservice
Gothenburg, Sweden 2010

Detection of Electrical Treeing in XLPE Exposed to AC and DC Voltage Stress
ANETTE B. JOHANSSON
ANNA-MARIA B. SANDBERG
Department of Materials and Manufacturing Technology
Chalmers University of Technology

Summary

For this master thesis work the main focus was to build an experimental setup, with a wire-plane electrode configuration, for detection of electrical treeing in XLPE exposed to DC voltage. A 50 Hz AC voltage was used for comparison with the DC results and with previous work.

The constructed high voltage circuit utilized a CCD camera for optical detection of electrical treeing and a half-wave bridge rectifier to supply the DC voltage. Two linear ramping speeds were analysed, both for positive and negative DC as well as for AC voltage. The wire-plane configuration was affirmed to be reproducible. For the DC tests it was found that complete breakdown of the XLPE would occur before any electrical trees could be discerned with the CCD camera. DC breakdown voltages were compared; negative polarity resulted in higher voltage levels than positive polarity. When comparing AC and DC stressed test objects it was found that the breakdown voltages, for both polarities of DC voltage, were distinctly higher than the treeing inception voltage for the AC stressed objects. Regarding the effect of voltage ramping speed it was seen that the faster ramping resulted in higher tree initiation field for AC stressed test objects and a lower breakdown voltage for the DC stressed test objects.

The specimens were inspected in a microscope and several types of tree structures were distinguished for both AC and DC.

Keywords: Electrical treeing, XLPE

Acknowledgements

This master thesis project was supported by ABB High Voltage Cables in Karlskrona and they are gratefully acknowledged for this.

First and foremost we would like to thank our supervisor Dr. Björn Sonerud for support and guidance throughout the ups and downs of our master thesis work. Secondly we want to show our gratitude towards our examiner Prof. Stanislaw Gubanski for his theoretical aid on insulating materials and his advice on the report. Andreas Farkas, our contact at ABB High Voltage Cables in Karlskrona has been a great help both for sharing his knowledge in this field and for arranging a trip to ABB, enabling us to use their microscope. Furthermore we want to thank Aleksander Bartnicki and Dr. Jörgen Blennow for sharing their time and experience helping us, especially when we had trouble with the experimental setup. We would also like to thank Dr. Villgot Englund, Borealis for teaching us the sample manufacturing process and the division of Polymer Technology at the Department of Chemical Engineering for allowing us to use their equipment and lunch room, with a special thanks to Patrik Henriksson and Susanne Nilsson for helping us. Finally we would like to thank Dr. Stefan Lundberg for advising us on the more practical aspects of safely using the equipment in the metal workshop.

Anette Johansson & Anna-Maria Sandberg

Göteborg, Sweden
2010

Table of Contents

Summary	iii
Acknowledgements	iv
Table of Contents	v
1 Introduction	1
1.1 Background	1
1.2 Purpose	1
1.3 Scope	1
1.4 Method.....	2
2 Literature Review	3
2.1 Electrical Trees.....	3
2.1.1 Initiation	3
2.1.2 Propagation.....	4
2.1.3 Runaway.....	6
2.1.4 Polarity Effects in Dielectrics under DC Stress.....	6
2.2 Electrode Configurations for Measuring Electrical Treeing Resistance	6
2.2.1 Preceding Electrode Configurations.....	6
2.2.2 The Newly Developed Wire Configuration.....	7
2.3 The Weibull Distribution.....	7
3 Sample Manufacturing	9
3.1 Pressing of Semiconducting Tabs	9
3.2 Pressing of Polyethylene Strips	10
3.3 Cross-linking of the Polyethylene while Moulded with the Semiconducting Tab.....	11
3.4 Finalizing the Test Samples.....	12
3.5 Kinks	13
4 Method.....	15
4.1 Experimental Setup	15
4.1.1 Electrical Circuits	15
4.1.2 Physical Arrangements	16
4.1.3 Optical Arrangements.....	18
4.2 Components.....	19
4.2.1 Voltage Dividers.....	19
4.2.2 Voltage Source	22
4.2.3 Capacitors.....	22
4.3 Transformer Oil.....	22

4.4 Signal Processing.....	23
4.4.1 LabVIEW Coordination with CCD Camera	23
4.5 Voltage Determination.....	23
4.5.1 AC Voltage Determination	24
4.5.2 DC Voltage Determination	26
4.6 Weibull Analysis.....	28
5 Results.....	29
5.1 Electrical Treeing Due to AC Stress.....	29
5.1.1 Comparison with Previous Work.....	30
5.1.2 Comparison of AC Tree Inception Voltages with Different Ramping Rates.....	31
5.1.3 Comparison of Tree Inception Voltages for Treeing at Wire vs. Treeing at Kinks	35
5.1.4 Breakdown Channel Formation during Tests with Applied AC Voltage	37
5.2 Electrical Treeing due to DC Stress.....	39
5.2.1 Breakdown Tests at Ramping Speeds of 5.3, -5.4 kV/s	40
5.2.2 Breakdown Tests at Ramping Speeds of ± 0.7 kV/s	47
5.2.3 Comparing the DC Results with the AC Results	51
5.3 Temperature Impact on the Results	54
6 Discussion.....	57
6.1 Kinks	57
6.2 Visual Limitations and Requirements.....	58
6.3 Silver Flakes.....	59
6.4 Accuracy of Voltage Measurements	59
6.5 AC Phenomena	60
6.6 DC Phenomena	61
7 Conclusions.....	63
8 Future Work.....	65
References.....	67

1 Introduction

This master thesis project has been made in cooperation with ABB High Voltage Cables, Karlskrona. Measurements of the resistance to electrical treeing in cross-linked polyethylene, XLPE, have been made. The electrical trees were also analysed in a microscope. The XLPE analysed has been provided by ABB High Voltage Cables.

1.1 Background

Polymeric material is nowadays a commonly chosen material as insulation of high voltage cables, due to excellent electrical, thermal and mechanical properties. Although with time, the electrical properties deteriorate when exposed to electrical stress. One of the main causes of degradation and breakdown in polymeric insulation material for high voltage systems is electrical treeing [1]. Accordingly research on the properties of electrical trees has been made since the 1950s [2]. With the introduction of HVDC power transmission systems the interest in electrical treeing due to DC stress has increased and research is ongoing in this area [3], [4]. Needle-plane, needle-rod and short cable specimens are commonly used for initiation of electrical trees, both for AC and different types of DC stress [5], [6], whereas the wire-plane configuration applied for this work has earlier been used in AC tests [7].

1.2 Purpose

The purpose was to design and build an experimental setup, using a wire-plane configuration, for optical detection of electrical treeing in XLPE exposed to a ramped AC and DC voltage. The treeing initiation field was to be compared for the two voltages and for both polarities of DC stress.

1.3 Scope

The priority was to achieve results when stressing the test objects with DC voltage. The exposure of 50 Hz AC stress was in order to compare the results with the previous work done by Huuva [7] and to have a reference to DC results achieved in this project. A slower and a faster ramping speed were investigated for both the AC tests and for positive and negative voltage polarity in the DC tests. The slower rate of 0.5 kV/s (rms) was chosen since it is specified in the ASTM standard D 3756 – 97 for tests of resistance to electrical breakdown by treeing [8], it was also used in the previous work [7] and was the lowest ramping rate of the available AC regulator. The faster ramping rate of 3.9 kV/s was decided while performing the tests, since it enabled experiments with applied DC voltage to be carried out without flashovers in the surrounding circuit.

There are five ways to initiate electrical treeing involving DC voltage; ramping, short-circuit (grounded), polarity reversal, impulse and constant voltage [9]. The first method was used in this project; ramped voltage for one polarity at the time. The other methods would require regulation of switches and a computerised control of the applied voltage.

This would have taken more time leaving less time to spend on performing experiments and analysing results.

The dielectric material, XLPE, used in this project was provided by ABB High Voltage Cables.

1.4 Method

Optical detection was implemented to study the behaviour of electrical treeing in XLPE. The test objects were of a recently developed wire-plane configuration. A high voltage test circuit was designed and setup. The XLPE was exposed to both AC and DC voltage, where the DC was achieved using a half wave rectifier. The experiments were performed in a high voltage laboratory at Chalmers University of Technology.

2 Literature Review

This chapter will describe how electrical trees are formed in a dielectric material. Some insight in preceding test arrangements for evaluating resistance to electrical treeing will be given whereas a more thorough explanation is presented for the newly developed electrode configuration which was used in this master thesis project. Finally the Weibull distribution, a statistical method for analyzing results, is explained.

2.1 Electrical Trees

Electrical treeing is a degradation phenomenon developing in dielectric insulation exposed to high electric fields. Partial discharges initiate formation of a tree-like structure and cause the tree to propagate and eventually cross the entire insulation thickness, thereby short-circuiting it.

This chapter will contain the physics of electrical treeing development, i.e. initiation, propagation and runaway. There is also some information about polarity effects related to DC tests.

2.1.1 Initiation

According to Dissado's review [10] the starting point for a tree growth is the injection of charges due to an electrode geometry producing high divergent fields or by gas discharge in voids. The evidence for this is the detection of electro-luminescence that appears before partial discharges (PDs). The first tubule of electrical trees is a product of a chain of events. The injected charges are accumulated and for a certain level it enables excitation of molecules from some kind of energy release. It might be due to; their kinetic energy, recombination of charges of opposite polarity or trapping [11]. The excitation or ionization enables bond breaking of the polymer chain due to chemical reactions which makes the final damage needed for the tree initiation channel [10].

The local field enhancement triggering a tree initiation can also be an effect of impurities though these play a smaller role today as insulation materials are cleaner with improved production methods [12]. There are also synergetic effects; if large amounts of impurities are present these tend to localize around large crystals. Together they create a worse case of weak regions than they would have done separately [13].

Mechanical properties such as tensile strength, elastic modulus and fracture toughness has been proven to influence both initiation and tree growth in polyester resin. A higher tensile stress, present in the insulation and produced during its manufacturing process, will give rise to a faster tree growth [14]. This analysis concerns the insertion of an electrode needle.

Temperature is another factor with a significant impact on electrical treeing. It can change a material's mechanical characteristics, thereby influencing tree initiation and growth [14]. Temperature has been proven to make a major reduction of times to breakdown in XLPE

[15]. Other properties affected by temperature are conductivity and morphology. Vaughan et al. demonstrated how a temperature increase from 20°C to 30°C would change the degeneration of polyethylene to carbonized residues with the effect of conducting tree channels [16].

2.1.2 Propagation

The propagation stage is defined to begin when discharges with a magnitude of 0.1 pC or higher can be detected. Tubules enabling this are thought to be at minimum 5-10 μm long and with a radius of 1 μm [10].

There are two main categories of electrical tree structures that are commonly referred to in literature; branch and bush. The names are given by their geometrical shapes, the bush tree being denser than the branch tree. They are attributed with different discharge rates and fractal dimensions [17], [18]. Branch trees propagate with a much higher rate than the bush [17]. Branched trees have a fractal dimension approximately between 1 and 2 for bush trees it varies between 2 and 3 [18]. A high value of the fractal dimension means that the fractal covers a space more extensively.

There are also differences in how branch and bush trees are formed. For starters, experiments have shown that bush tree formation needs higher electric field strengths than branch tree formations [9]. Then, the actual physics behind the propagation deviates. For branch-trees the channel becomes conducting due to graphitic deposits and it will suppress partial discharges to take place inside the channel [16]. At the same time charges are injected into the solid building a net space charge resulting in a high local field at the tip of the channel. As a consequence partial discharges arise at the channel tip and with the thermal energy released from the discharges there is energy enough to degenerate the insulation further [17]. The branch tree will extend in this way by stepwise breakdown of the dielectric material.

The first channel of a bush tree is started as that of a branch tree. Then branching will continue as a result of partial discharges throughout the tree, from the electrode tip to the channel end [10]. This is enabled by the lack of conducting particles on the walls, i.e. there is enough resistance for a voltage drop inside the channel [16]. Due to more branches created from channels close to the electrode the bush will have a dense structure. Branches might also be created by large amounts of charge on the channel walls which make extensions possible from the side and with this growth it neutralises the channels from charge [9].

The reason that discharges disappear in a channel has been associated with both an increased conductivity of the channel walls [16], [17] and an increase of gas pressure [10], [17]. Though, since partial discharges are the cause of increased pressure a suppression of discharges would result in a pressure decrease, which in turn would increase the discharges all over again. In other words there will be equilibrium, not a total extinction of partial discharges [15]. Also, Laurent and Mayoux argued in 1980 that some channels in their experiments had reached the dielectric surface, which would have decreased the pressure but the discharges would not increase, thereby indicating the gas pressure not to be the cause, at least alone, for discharge extinction [17].

DC tree growth has not been that well discussed in literature. Dissado and Fothergill made a description of DC trees being propagated by avalanches and that due to the homo-charge injection only branch-tree structures will be formed [9].

Tree shapes that will be mentioned in this master thesis work are bush, branch, mirror-trees, mini-trees and filaments. Again it has to do with their geometric shapes, see Figure 2.1 for an overview of the tree-types. The mirror-trees have been named for their growth towards both the grounding electrode and the high voltage potential. The difference between the mini-trees and the filaments are that the filaments are even smaller and have shorter branches. The filaments were also found in abundance whilst the mini-trees were found individually growing.

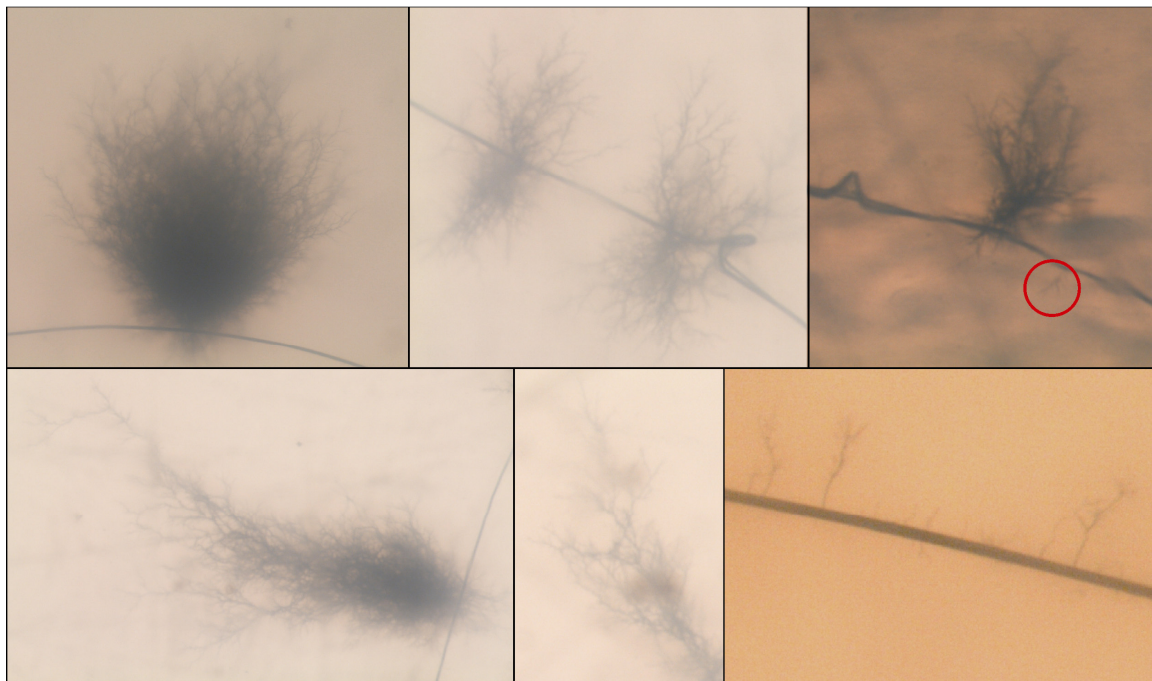


Figure 2.1 Overview of tree-shapes. Top, from left; bush, mirror and mini (encircled). Bottom, from left; bush-branch, branch and filaments.

There are different opinions on whether the geometry and the material of the electrode will have any influence on the propagation phase. Zheng and Chen stated in year 2008 that the material will only involve the initiation of trees [2]. Ieda and Nawata on the other hand presented an experiment in year 1977 in which the material of the inserted electrode would alter the tree length. Materials with a smaller work function would more easily inject charges and so the trees become longer. It should be noted that the relation between tree length and electrode material could only be seen with applied negative prestress voltage [6].

It is also believed that branch trees develop in a more chaotic way while bush trees are in whole deterministic. There are many complex forms of trees but those regarded as bush type will more or less get the same structure according to Dissado et al. [10].

Electrical trees developed during AC stress are dependent on applied voltage frequency; the higher frequency the shorter time to breakdown [1] and a higher frequency also lowers

the field strength needed for treeing initiation [9]. This, explained by Ieta and Nawata in 1972 (cited in [1]), is due to the higher amount of repeated gas discharge taking place inside the tree tubules.

2.1.3 Runaway

The acceleration stage occurs when a tree is close to crossing over the material to the other electrode. It is still not clear how the acceleration is triggered. One explanation is that when the propagation has ceased discharges may still be present in the tree, making the channels wider. With larger voids bigger discharges are possible and this together with the second electrode being close might give a sufficiently high electric field at the branch tip, giving rise to the accelerating growth [10].

2.1.4 Polarity Effects in Dielectrics under DC Stress

In experiments using needle-plate configuration and a DC voltage ramping rate of 0.5 kV/s a positive polarity results in lower tree inception voltage than for negative polarity. The trend has been proven for both impulse voltage and DC voltage with dielectrics such as LDPE, ethylene-vinyl acetate (EVA) and XLPE [3]. It is also a consistent result for different ramping rates for needle-plate arrangements with LDPE as dielectric material [6].

The polarity effect is caused by space charge built up around the needle tip [3]. The difference of the two applied voltages is the amount of charge injected by the electrode, negative polarity exceeding positive. The charges extend the needle and increase the effective radius of the needle tip which in turn reduces the electric field. It therefore takes a higher voltage for a tree initiation with negative polarity [19].

2.2 Electrode Configurations for Measuring Electrical Treeing Resistance

The most commonly used electrode configurations for initiation of electrical trees in solid dielectric material is presented together with the newly developed wire-plane arrangement.

2.2.1 Preceding Electrode Configurations

According to the ASTM standard test method from 2001 for evaluating resistance to electrical breakdown by treeing in solid dielectric material a needle-rod configuration is used [8]. The steel electrodes have a diameter of 1 mm and are moulded into 6 mm thick insulation. The needle curvature has a radius of $3 \pm 1 \mu\text{m}$ and an angle of 30 ± 1 degrees. For determining the voltage level of tree inception, the distance between the electrodes is controlled to 12.0 ± 0.5 mm. The voltage source refers to an AC with a frequency of 50 or 60 Hz.

The standard method is not always followed in the literature. Besides the needle-rod configuration there are needle-needle and needle-plane arrangements. Another electrode material that has been used is tungsten [2], [14]. The radius of curvature of the needle has been described to be between $1 \mu\text{m}$ and $5 \mu\text{m}$ [3], [14]. A drawback with these setups is the

formation of small voids at the needle tip when inserting it into the polymer. If a void is formed, partial discharges present in the cavity might initiate an electrical tree, which will not represent the material properties. Another disadvantage is that the tip of the needle might be deformed during the preparation of the samples, thereby changing the tip curvature and hence the electric field.

2.2.2 The Newly Developed Wire Configuration

In order to decrease the number of discarded samples a new electrode configuration has recently been developed at Chalmers University of Technology [7], utilising a thin tungsten wire as the high stress electrode rather than the commonly used needle. By employment of this method the problem with voids formed in the insulation material at the inserted needle tip is reduced [20]. Tungsten was chosen for its high elastic modulus and hardness as well as its low thermal expansion. The test object consisted of a semiconducting cross-linked polyethylene tab with a sewn on wire, having a diameter of 10 or 20 μm . The tab was moulded between two pieces of the polymer investigated. Two insulation materials were studied, XLPE and LDPE. As there were no field models available for this configuration of stress electrodes; the evaluation of the electric field strength at the wire, where the tree will originate, was simulated with Comsol Multiphysics Package [21]. By the use of the electric field strength, results can be compared with other kinds of electrode configurations. The accuracy of the relation might though be discussed since it does not take injected charges which will affect the electric field into consideration. It was also concluded that the results for different wire diameters did not agree perfectly when related to field strength, which was explained to be a consequence of only simulating the Laplacian field [7].

In this preceding study a 75kV, 50 Hz transformer was used to energize the sample. For optical detection of the electrical trees a CCD camera was used. The camera was triggered from a computer, which also registered the voltage. The picture frames were then stored for later analysis. Special attention was made to achieve an as corona free environment as possible. The voltage was ramped at a constant rate of 0.5 kV/s. When the tree spanned half the distance between the wire and the ground plane, the voltage was switched off. In this way the tree initiation voltage as well as the development of the electrical tree over time was studied. This new electrode configuration was found to be successful alternative to the common single needle and double needle configurations and was used for analyzation of LDPE and XLPE with and without different voltage stabilising additives.

2.3 The Weibull Distribution

The Weibull distribution is commonly used for describing breakdown phenomena in solid dielectric materials [22], [23]. This is an extreme value probability, with a wide applicability, where the system fails when its weakest link fails [23]. For data to be considered Weibull distributed it must be above a finite threshold. The threshold should have a physical meaning, as to why breakdown cannot occur below it. Normally it is desirable to have a large set of data when analyzing the statistical characteristics, this might be unreasonably expensive or problematic to achieve. Often a small number of samples are investigated and these are to form the basis of the analysis. Failure data

should be secured for at least ten test objects if possible, in order to provide a satisfactory estimation. With less than five test objects evaluated serious errors can be produced [24].

The three-parameter Weibull distribution consists of the following parameters: the scale parameter, $\alpha > 0$; the shape parameter, $\beta > 0$; and the threshold parameter, $\gamma \leq x$. x is the variable measuring the failure rate, e.g. the breakdown voltage or the time to breakdown. The cumulative probability function is then given by Formula 2.1:

$$F(x; \alpha, \beta, \gamma) = 1 - e^{-\left[\frac{x-\gamma}{\alpha}\right]^\beta}; \quad x \geq \gamma \quad (2.1)$$

The probability of failure is zero when $x=\gamma$. The cumulative probability function increases together with x and approaches one, as x approaches infinity. The scale parameter, α , represents a failure rate of $1/e$ or about 0.632. The scale parameter is analogous to the mean of the Normal distribution. The shape parameter, β , indicates the range of the measured variable. A large β corresponds to a narrow range. The threshold parameter, γ , is a finite lower limit, such that the probability of failure for $x < \gamma$ is zero.

A special case of the three-parameter Weibull distribution is the two-parameter adaptation, where γ is set to zero. Formula 2.2 shows the cumulative distribution function of the two-parameter Weibull distribution:

$$F(x; \alpha, \beta) = 1 - e^{-\left[\frac{x}{\alpha}\right]^\beta}; \quad x \geq 0 \quad (2.2)$$

When all samples in a test give relevant breakdown values the data is called uncensored or complete, if a part of the samples for some reason are omitted from the evaluation the data set is considered censored. Samples may be excluded for several reasons e.g. if the sample withstands the maximum voltage of the test or if the breakdown is due to another breakdown mechanism than the one studied.

The maximum likelihood estimator (ML) and linear regression using least squares (LSR) are two common methods in estimating α , β and γ . There are also a number of more complex estimation techniques such as; the White estimator, the Jacquelin estimator and the Bain-Engelhardt [25]. These provide a more correct estimation of the Weibull distribution for a small number of data; with more collected failure data the ML and LSR become comparable in accuracy.

3 Sample Manufacturing

The samples used for the experiment were composed of a semiconducting tab, a 10 μm tungsten wire and an XLPE insulation material from ABB High Voltage Cables in Karlskrona. There was no information provided about the type of XLPE, whether it for example contained voltage stabilizers or not. The wire was sewn onto the semiconducting tab, leaving a projecting half-circle at the top. This construction was then pressed between two polyethylene strips to form one entity, using a Fotinje press. During this process the cross-linking of the polyethylene took place. The dimensions of the test object are shown in Figure 3.1.

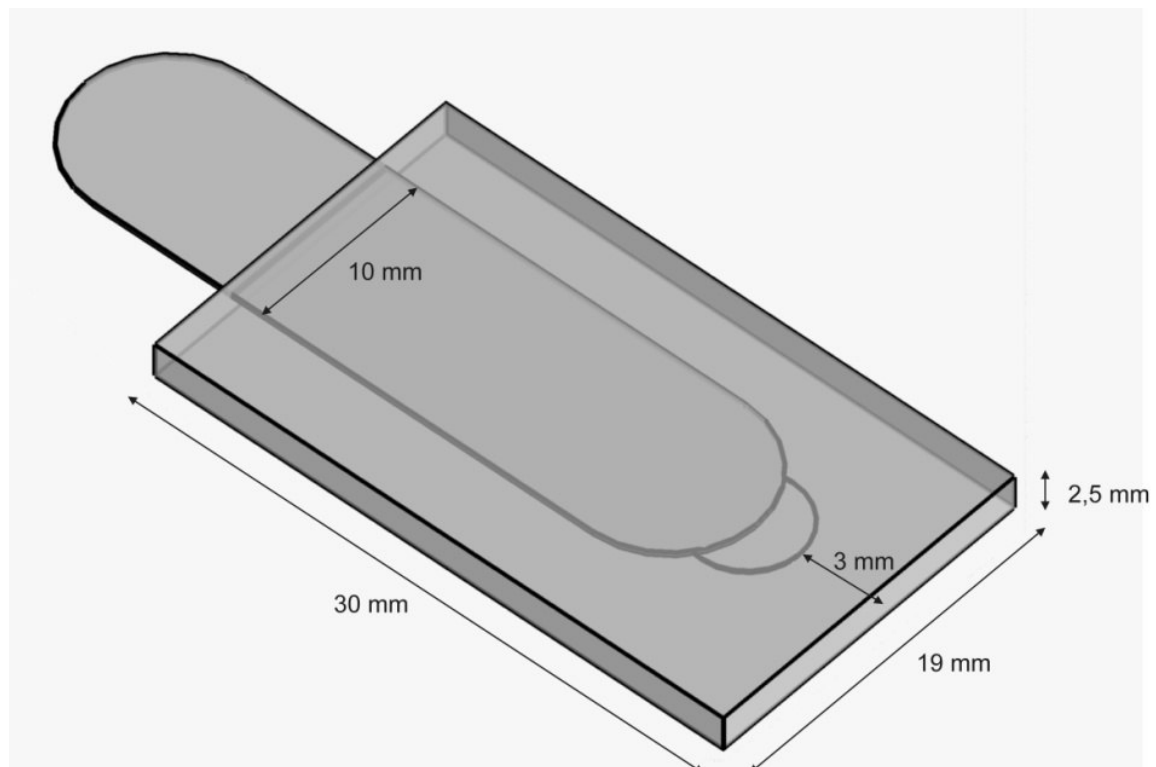


Figure 3.1 Test object with its dimensions.

3.1 Pressing of Semiconducting Tabs

The semiconducting tabs were manufactured from a grounded polyethylene powder. Around 10 g of powder was spread between two plastic films in between two plates which were placed in the press when the temperature had reached 130°C. At this temperature the semiconducting material was first exposed to a pressure of 2 kN for 3 minutes to melt the powder, this was followed by another 3 minutes with 200 kN of pressure. Then the temperature was raised to 180°C with a ramping time of 15 minutes. The temperature and pressure were kept for 15 minutes during cross-linking process. Finally, the temperature was decreased to ambient temperature with the pressure unchanged. The pressing scheme can be seen in Figure 3.2. After the pressing tabs were punched from the disc formed.

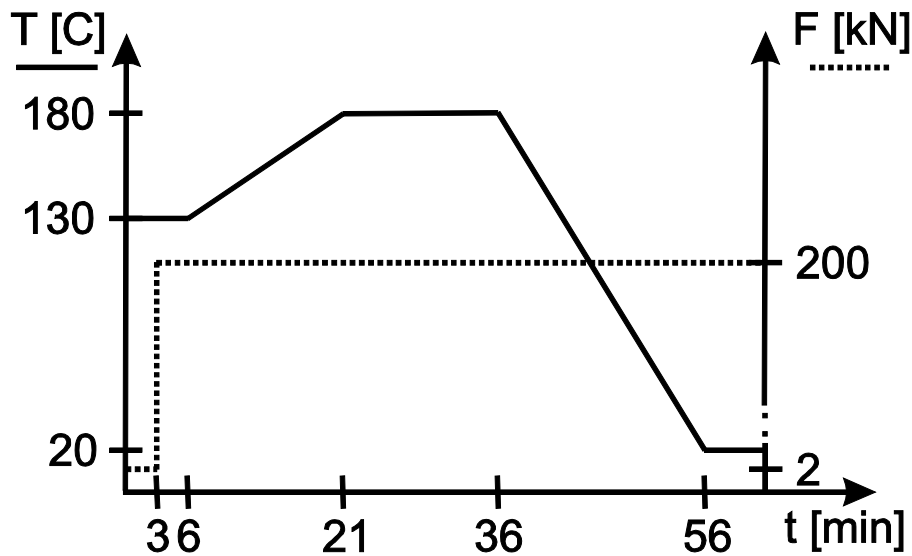


Figure 3.2 Pressing scheme for the semiconducting tab manufacturing process.

3.2 Pressing of Polyethylene Strips

The polyethylene insulation material was provided as pellets. These were cooled by liquid nitrogen to prevent the pellets from melting as they were pulverised, using a Retsch grinder. Approximate 15 g of polyethylene powder was used to fill a metal mould for five strips. The pressing scheme for the polyethylene strips can be seen in Figure 3.3. The pressure was 2 kN at the start of the process with a temperature at 130°C. After 3 minutes the pressure was raised to 200 kN and the pressure was kept for 3 minutes before the temperature was decreased to room temperature of around 20°C which took about 15 minutes.

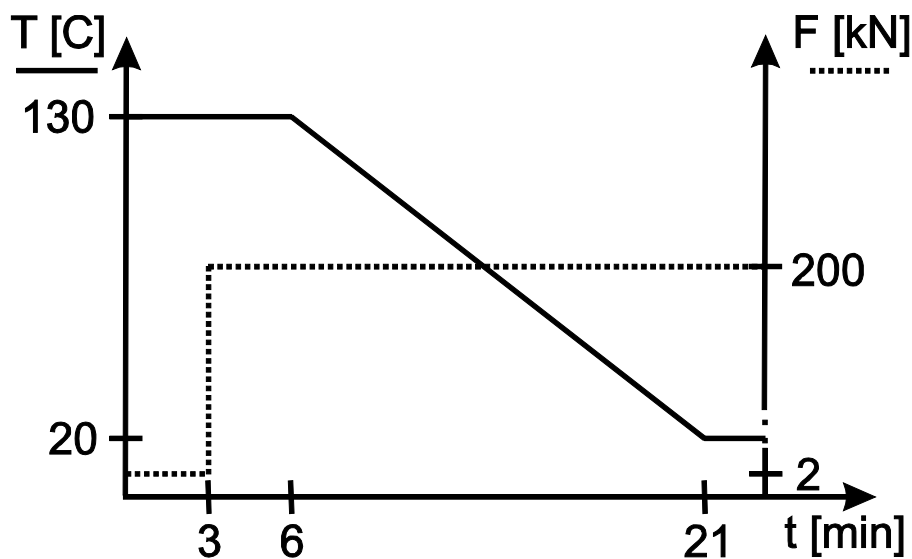


Figure 3.3 Pressing scheme for the polyethylene strips manufacturing process.

3.3 Cross-linking of the Polyethylene while Moulded with the Semiconducting Tab

The semiconducting tabs, with the tungsten wire attached, were placed between two strips of polyethylene insulation and then pressed together according to the scheme seen in Figure 3.4. A pressure of 2 kN and a temperature of 130°C was used the first 15 minutes. It was followed by ramping the pressure during 15 minutes up to 200 kN, the pressure was kept for the remaining part of the program. During the ramp of the pressure, the temperature was raised to 180°C. This was then kept for 15 minutes as the cross-linking of the polyethylene took place. As a final step the temperature was decreased to ambient during 30 minutes.

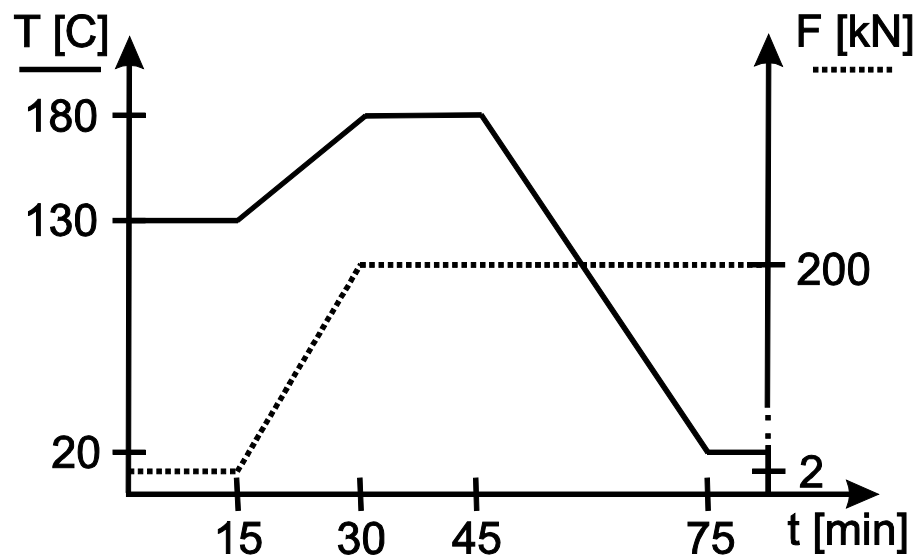


Figure 3.4 Pressing scheme for the cross-linking and joining process.

The test samples before the joining process is made are shown in Figure 3.5. The metal moulds were placed between plastic films and metal plates. These were the same moulds as used when pressing the polyethylene strips. The discoloured spots on the metal forms could not be removed and are assumed not to affect the sample quality.

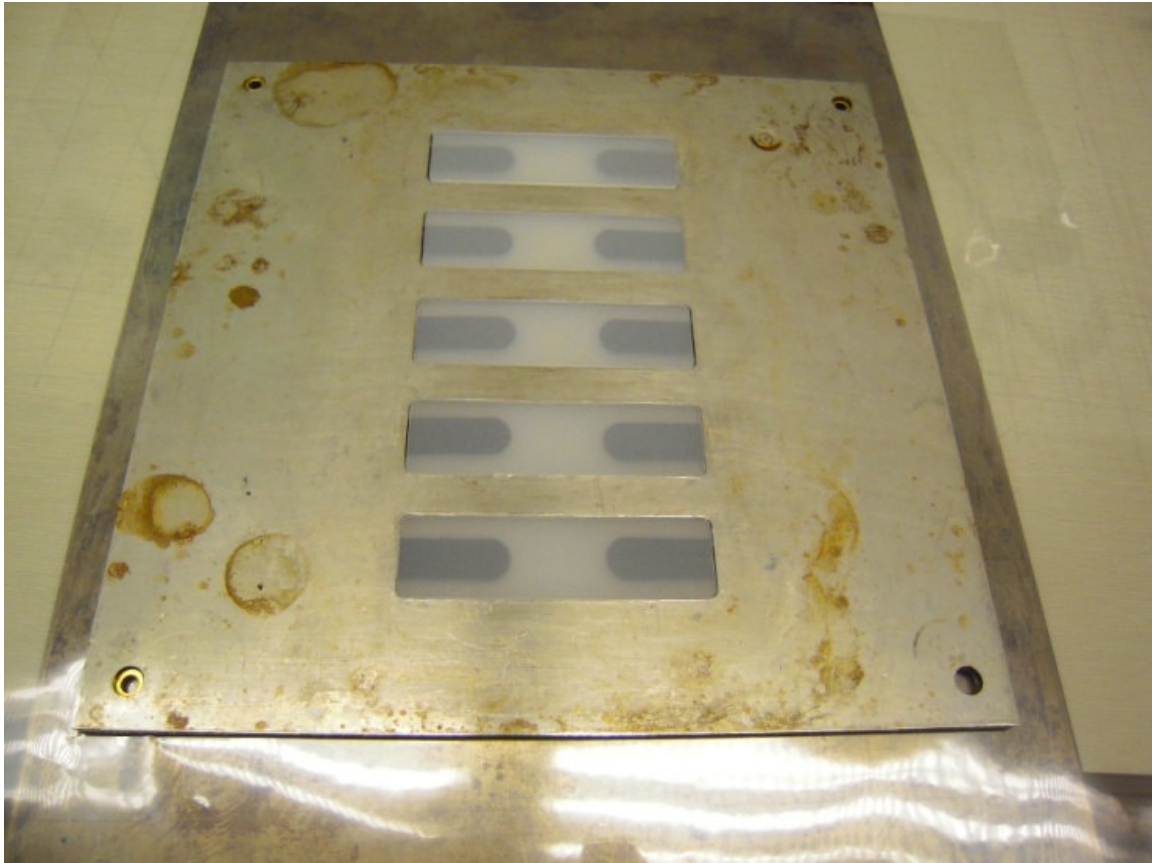


Figure 3.5 Test objects placed in the metal mould. Below one of the metal plates and a plastic film can be seen.

3.4 Finalizing the Test Samples

The cross-linking process of polyethylene produces byproducts such as; methane, acetophenone and cumylalcohol [26]. These fill voids thereby changing the morphology of the insulating material. The presence of byproducts will result in a higher resistance to electrical treeing [10], [26]. They will evaporate from the material and are not present in the material as it has been in use for some time. This process is speeded up to make the tests more reliable, by achieving the end product of a degassed material. To remove the byproducts the samples were placed in a vacuum desiccator during five days at a temperature of 60°C.

Finally the samples were cut at a 3 mm distance from the wire to create the plane electrode. This was painted with silver to secure a good grounding of the electrode by avoiding an oil film between the ground plane and the XLPE. Another reason for this was to have test objects analogous to those used in the previous work with the same electrode configuration [7]. In Figure 3.6 a completed test object is shown together with a close-up of the semiconducting tab with sewn wire.

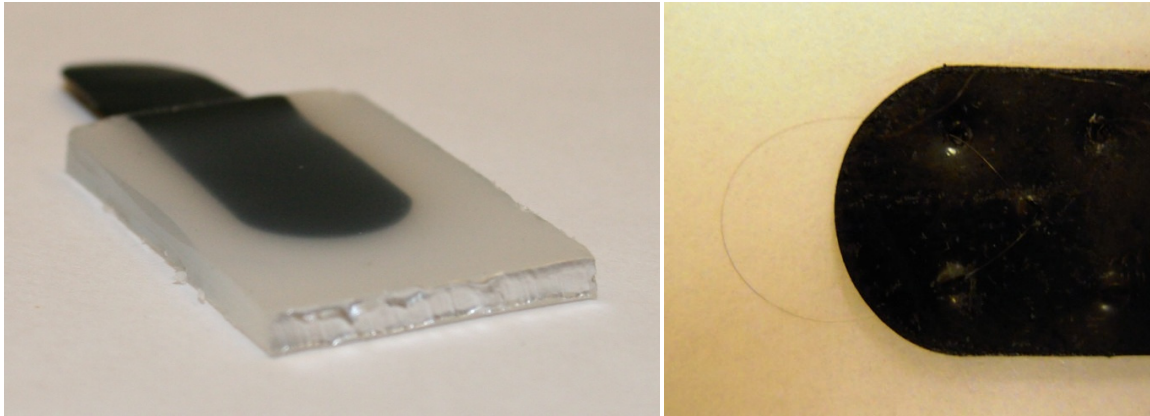


Figure 3.6 View of a test sample and close-up of 10 μm wire electrode.

3.5 Kinks

It was known from the previous work that the wire could form kinks, see Figure 3.7, during the manufacturing process although not to what extent they developed. It was thought to only appear occasionally so no particular precautions were taken. To be able to see a kink a microscope is needed, which was not available at the time of the sample manufacturing. Later on, kinks were discovered in different amounts and different shapes for more or less every test object. The effects of kinks for electrical treeing will be presented in Chapter 5.1.3.

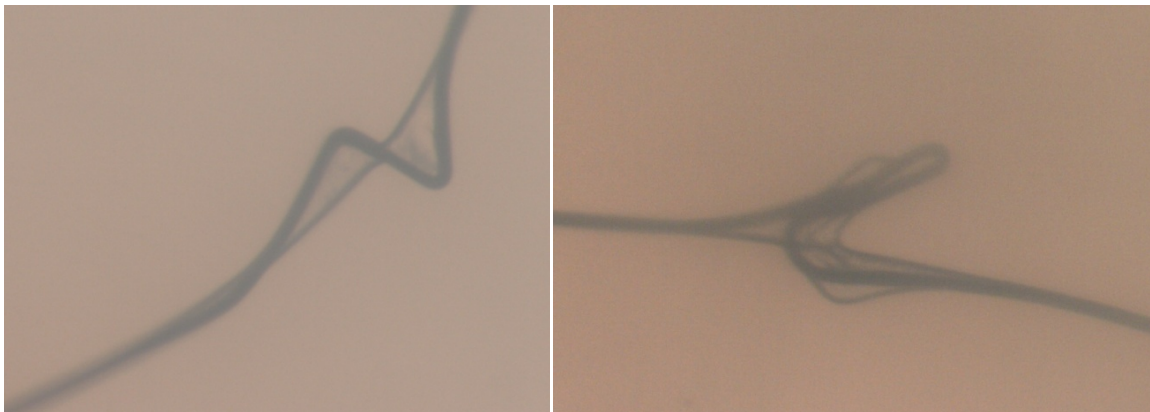


Figure 3.7 Left: *Split wire seen in a kink of an untested reference sample.* Right: *The wire forming a kink in one of the tested samples.*

The kink seen in the left hand picture of Figure 3.7 was found in a reference sample. This sample has not been subjected to any voltage stress, in other aspects it does not differ from the other test objects. The right hand picture shows a kink in a tested sample. From Figure 3.7 it seems as if the tungsten wire has split itself both for the reference specimen and the test object stressed by high voltage.

4 Method

The high voltage circuit built is described, together with its different components. Also the optical detection as well as the signal processing of the measurements are explained in this chapter.

4.1 Experimental Setup

The laboratory setup is described focusing on the electrical, optical and physical aspects.

4.1.1 Electrical Circuits

In this part the electrical circuits representing the setup arrangements for applied AC and DC voltage are displayed. The AC voltage levels are represented as rms values.

4.1.1.1 AC Circuit

The AC circuit consisted of an AC transformer connected to the test object through a water resistor of around 200 k Ω , acting as a current limiter in case of a breakdown. For the first set of tests, at the lower ramping speed of 0.5 kV/s, a capacitive voltage divider was connected in parallel with the test object. This was later changed to a resistive voltage divider for the test with the ramping speed of 3.9 kV/s. An electric schematic of the AC circuit is shown in Figure 4.1.

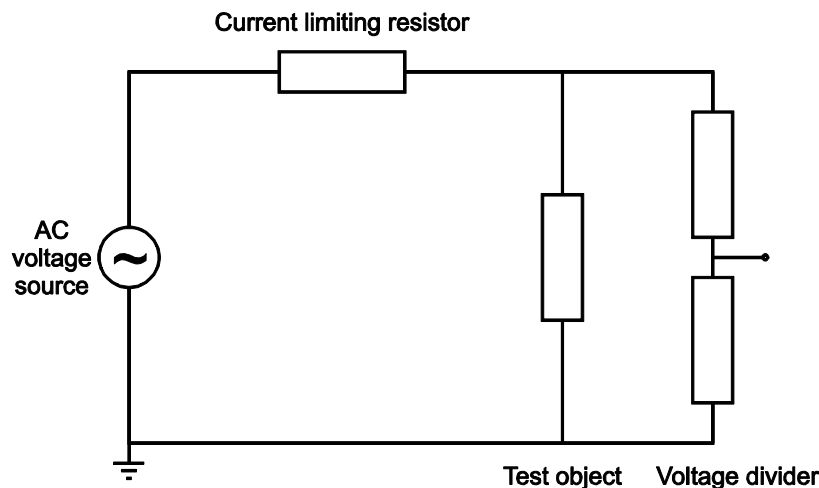


Figure 4.1 *The AC circuit.*

4.1.1.2 DC Circuit

A half-wave bridge rectifier was used to convert the AC voltage to a DC voltage. The AC setup was adapted by adding a diode together with a smoothing capacitor. The capacitor was used to decreasing the ripple and it lifted the DC voltage magnitude to the peak voltage level of the AC source. A second water resistor of around 150 k Ω was connected in series with the diode to prevent short-circuiting through the capacitor when the voltage is

switched on before the capacitor is energized. A resistive voltage divider was used for measuring the DC voltage at the test object. The schematic of the DC circuit can be seen in Figure 4.2.

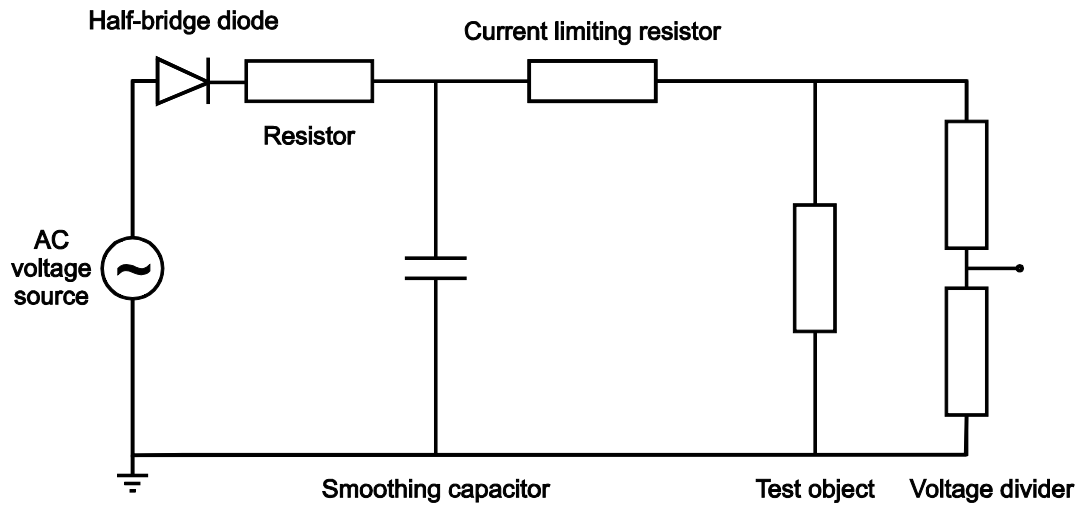


Figure 4.2 The DC circuit.

4.1.2 Physical Arrangements

The floors was covered with copper sheets and served as grounding plane. All grounding wires for external components were connected to the copper floor, which in turn was connected to common ground. A large post insulator stabilised the larger conductor (75 mm in diameter) connected between the AC transformer and the water resistor. A smaller post insulator held the T-connection of the smaller conductors (45 mm in diameter) connecting the lower part of the water resistor, the voltage divider and the test object holder. All these parts of the setup can be seen in Figure 4.3. The red/beige cylinder at the right part of the picture is part of the capacitive voltage divider used for the 0.5 kV/s AC stress. One can also see the aluminium foil wrapped around joints, for example at the top of the water resistor and at the T-connection, used to avoid sharp edges, thereby reducing the amount of partial discharges in the circuit. For the same purpose blu-tack, a semiconducting paste, was attached to the cables ties that fixated the high voltage conductor onto the wooden frame. The grey metallic wall in the background was grounded and an adequate distance from components with high voltage potential was kept.

Figure 4.4 shows the DC setup which is based on the AC setup. This picture was taken between tests, which is why the camera is not in a proper position. Starting from left in the picture; the AC transformer is here connected to the diode giving a positive polarity of the voltage, then follows the small water resistor and the capacitors which in turn are connected to the large water resistor and finally to the voltage divider and the test object. The “third resistive voltage divider” is connected in parallel to the test object; see Chapter 4.2.1.1 for information about the voltage dividers.

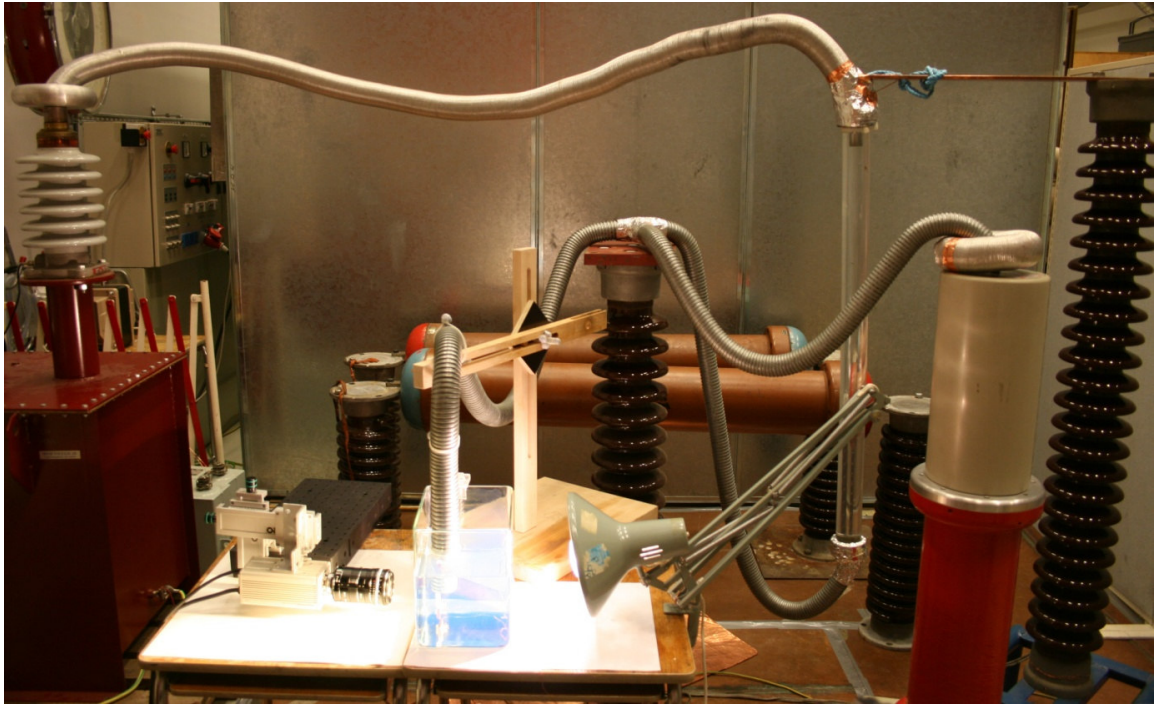


Figure 4.3 *Experimental setup for the AC tests.*

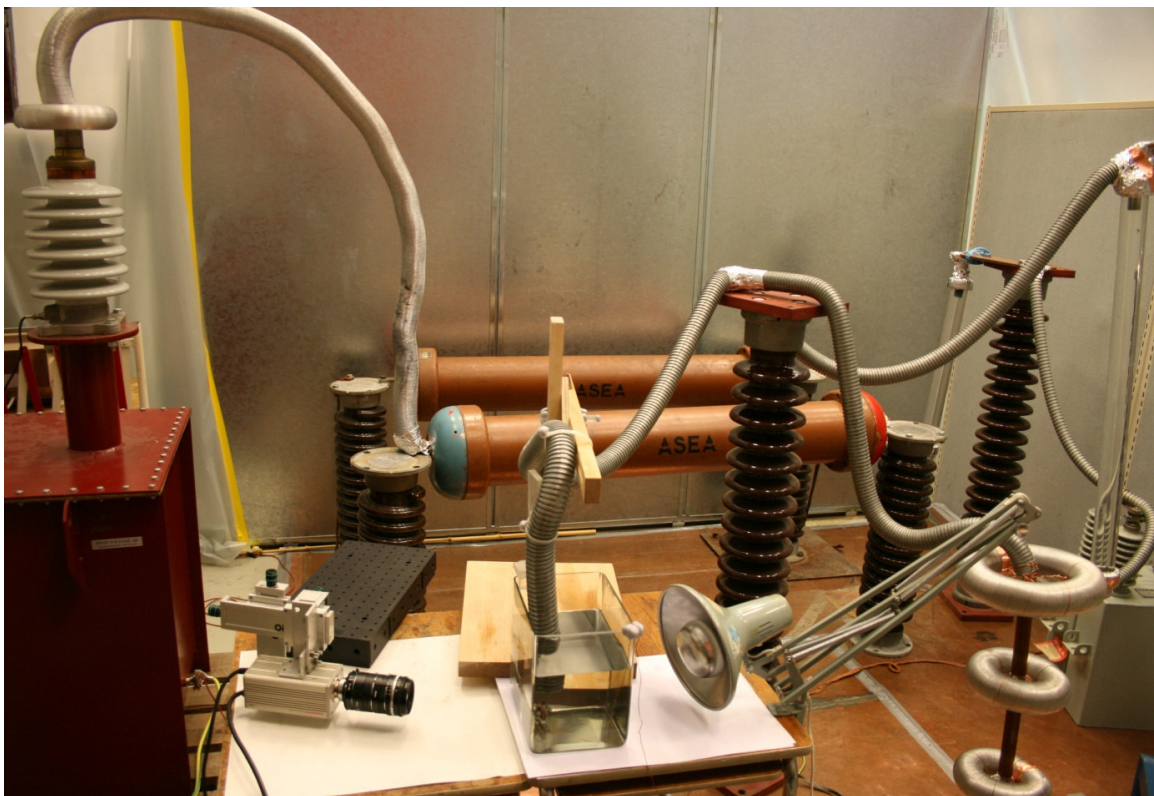


Figure 4.4 *Experimental setup for the DC tests.*

The test object was held with a pair of tweezers connected to the high voltage conductor, see Figure 4.5. The tweezers pressed the sample against a copper bar which was connected to ground with the seen in the background of the picture. Problems described later regarding flashovers between the conductor and the grounding wire during DC tests refers to this wire. These flashovers usually took place above the transformer oil between the

high voltage conductor and the ground wire, where it was bended over the edge of the aquarium.

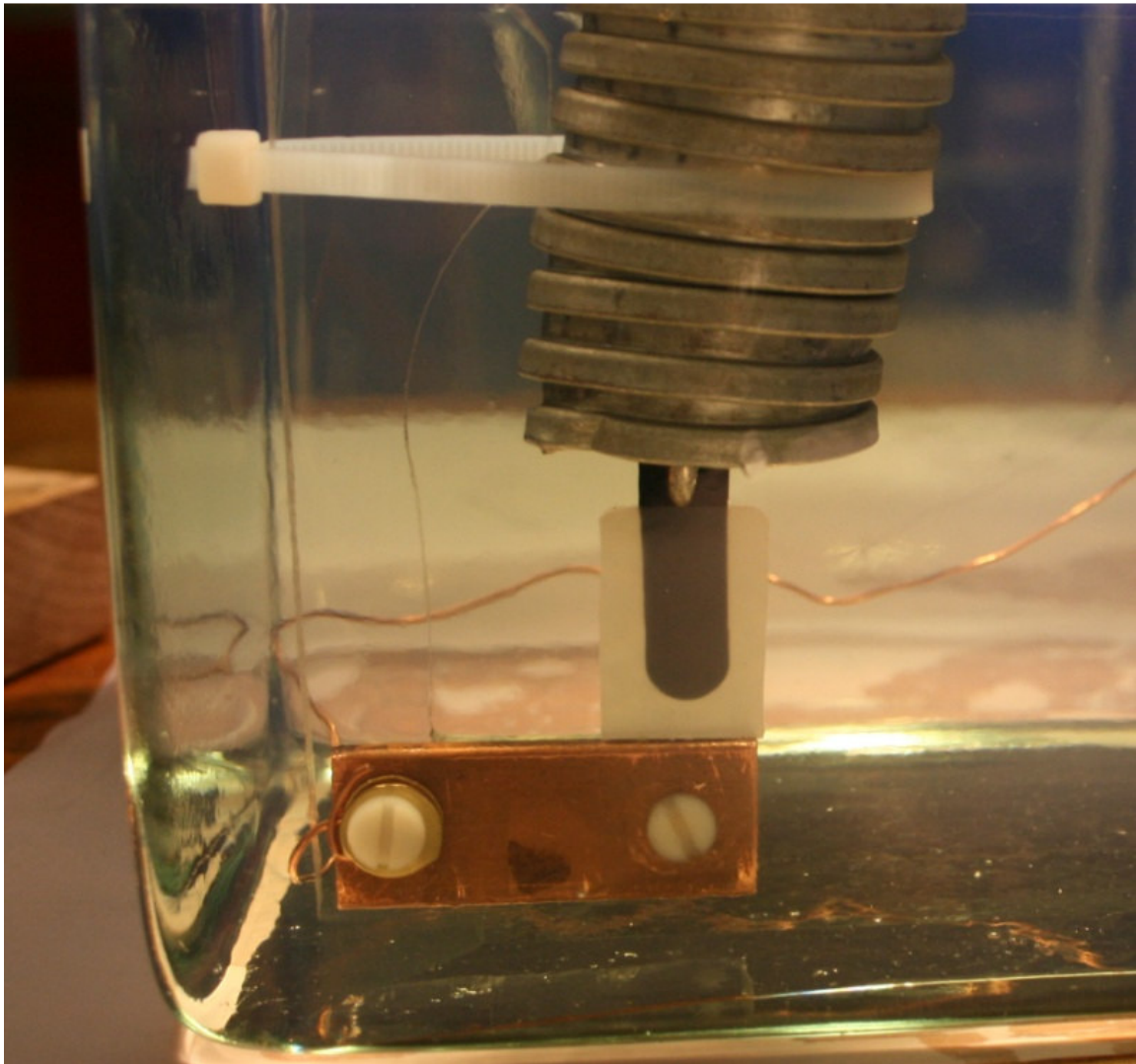


Figure 4.5 *Close up of test sample arrangement.*

4.1.3 Optical Arrangements

The test object was placed in an aquarium filled with transformer oil to prevent flashovers across it. A CCD (charge-coupled device) camera was used for recording optical images of the electrical treeing inside the test object. A Hamamatsu C5985 CCD camera, capturing 25 images per second, was used for this. The CCD camera was positioned in front of the test object, which was lit from behind to increase the contrast and enable a short shutter speed. A normal desk top lamp was used for this purpose with a reflector light bulbs of 150 W. White papers were also placed beneath the aquarium to reflect the light for even better lighting conditions. The optical arrangement consisting of the camera, the test object, the aquarium and the lamp can be seen in Figure 4.6.

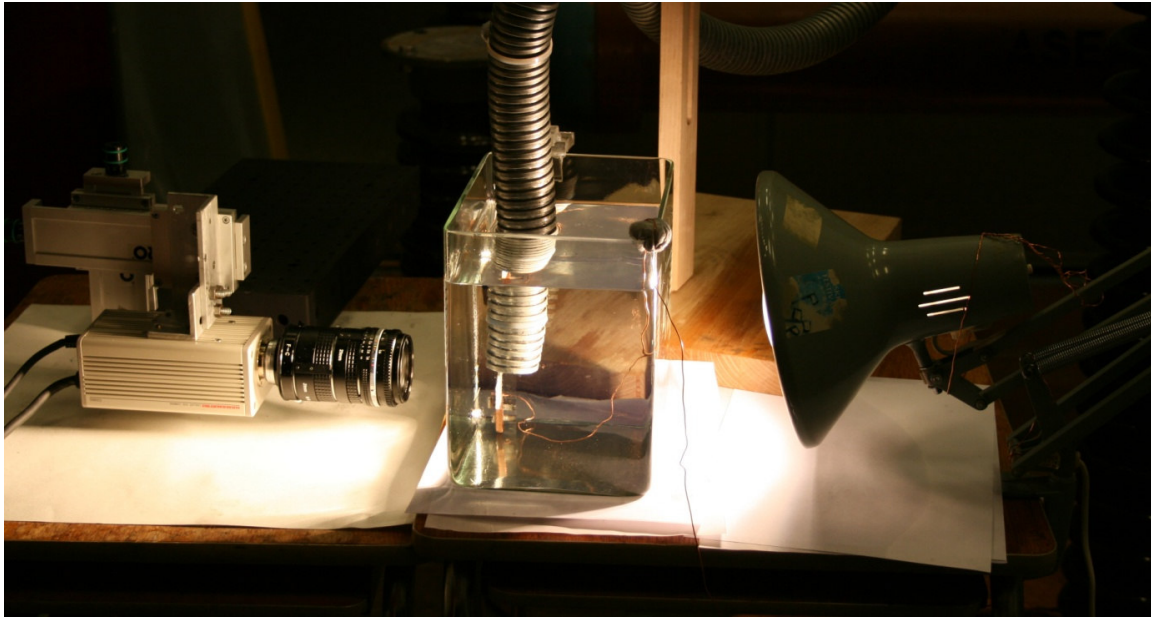


Figure 4.6 *Close up of the optical arrangements.*

4.2 Components

The voltage dividers were constructed specifically for this project and are further described in this part together with the voltage source and the capacitors.

4.2.1 Voltage Dividers

The inbuilt voltmeter of the AC source was not considered to be accurate enough and it provides the voltage level at the transformer instead of at the test object as was desired. For the purpose of attaining measurements of the voltage across the test object, a voltage divider was constructed. The analog input voltage of the DAQ, data acquisition device, should be kept in the range between -7 V to 7 V . To secure a safety margin the input voltage was kept between -5 V and 5 V . With the 16-bit analog-to-digital converter the resolution of the voltage measurement was $153\text{ }\mu\text{V}$.

Several different designs of voltage dividers were used. A resistive voltage divider was first attempted, which was meant to be used throughout all the tests. AC tests were the first ones to be carried out, but due too much partial discharge in this divider a capacitive voltage divider was used in this set of AC tests. The partial discharges were due to faulty design discovered later as the first voltage divider broke down. After completing the first set of AC tests a second resistive voltage divider was constructed to be used in the DC tests. Although also this voltage divider broke down, probably since it was used at voltage levels close to the rated maximum and a third resistive voltage divider had to be made. This divider in turn was used for measuring the voltage for the remaining DC tests and the second set of AC tests.

4.2.1.1 Resistive Voltage Dividers

Before it broke, the first faulty resistive voltage divider was used only when analysing the behaviour of the circuit and is thus not further described.

Resistive Voltage Divider - Second Design

The voltage across the small resistance for the maximum voltage supplied by the transformer was designed to be 5 V at maximum voltage. Three resistors, 94 M Ω , 100 M Ω and 8.2 k Ω were connected in series to achieve this. The peak voltage provided by the transformer of 106 kV results in a maximum voltage level across the low voltage resistor is 4.48 V. The high voltage resistors were rated for a voltage level of 50 kV each and were mounted vertically on top of an aluminium alloy box, covered by a plexiglass sheet for electrical isolation between the resistors and the box. To control the influence of stray capacitance in the voltage divider and to reduce partial discharges, two aluminium covered toroids were used as field grading rings. One field grading ring was placed on the top of the voltage divider and the other was used around the connection between the two high voltage resistors where sharp edges were present. The field grading rings had a diameter of 64 mm. The low voltage resistor was soldered, in parallel with a spark gap having a breakdown voltage of 75 V, inside the grounded box that acted as a mechanical support and limited the influence of the electric field on the low voltage signal. A BNC coaxial connector was attached where the voltage signal was measured. At the input of the BNC adapter, on the other side of the coaxial cable, two zener diodes were connected. The spark gap and diodes were connected in parallel with the small resistor for protection the BNC adapter and the DAQ in the case of an overvoltage. The resolution of the measured voltage was 3.6 V. The electric schematic is shown in Figure 4.7 and a photo of the second voltage divider is shown to the left in Figure 4.9.

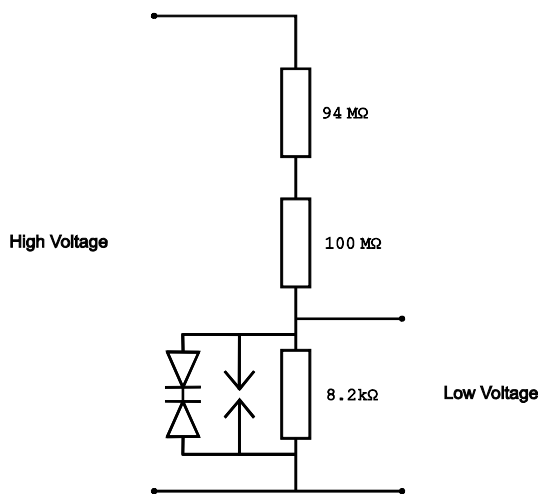


Figure 4.7 Schematic of second voltage divider with overvoltage protection.

Resistive Voltage Divider –Third Design

The third voltage divider was constructed with three high voltage resistors to decrease the voltage across them. To achieve the same voltage division the value of the low voltage resistor was changed to 13 k Ω . The high voltage resistors were measured to 100, 94 and 101 M Ω . A third field grading ring was also added. This resistive divider gave a resolution of 3.5 V of the voltage measurement. The electric schematic is shown in Figure 4.8 and a photo of the third voltage divider can be seen to the right in Figure 4.9.

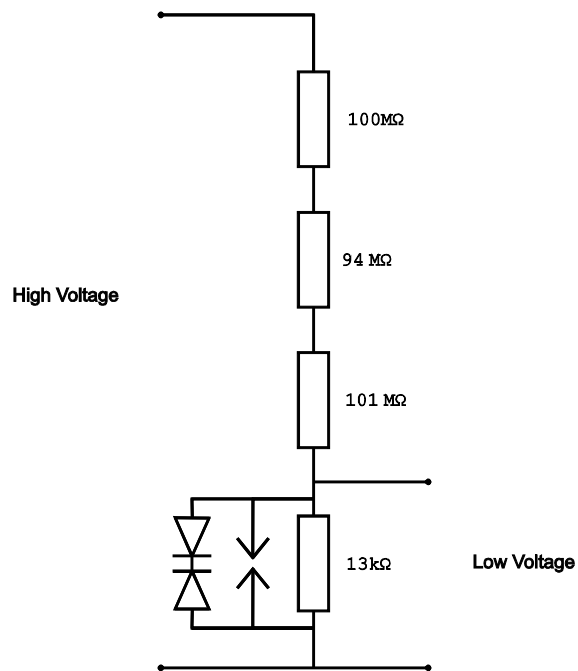


Figure 4.8 Schematic of third voltage divider.

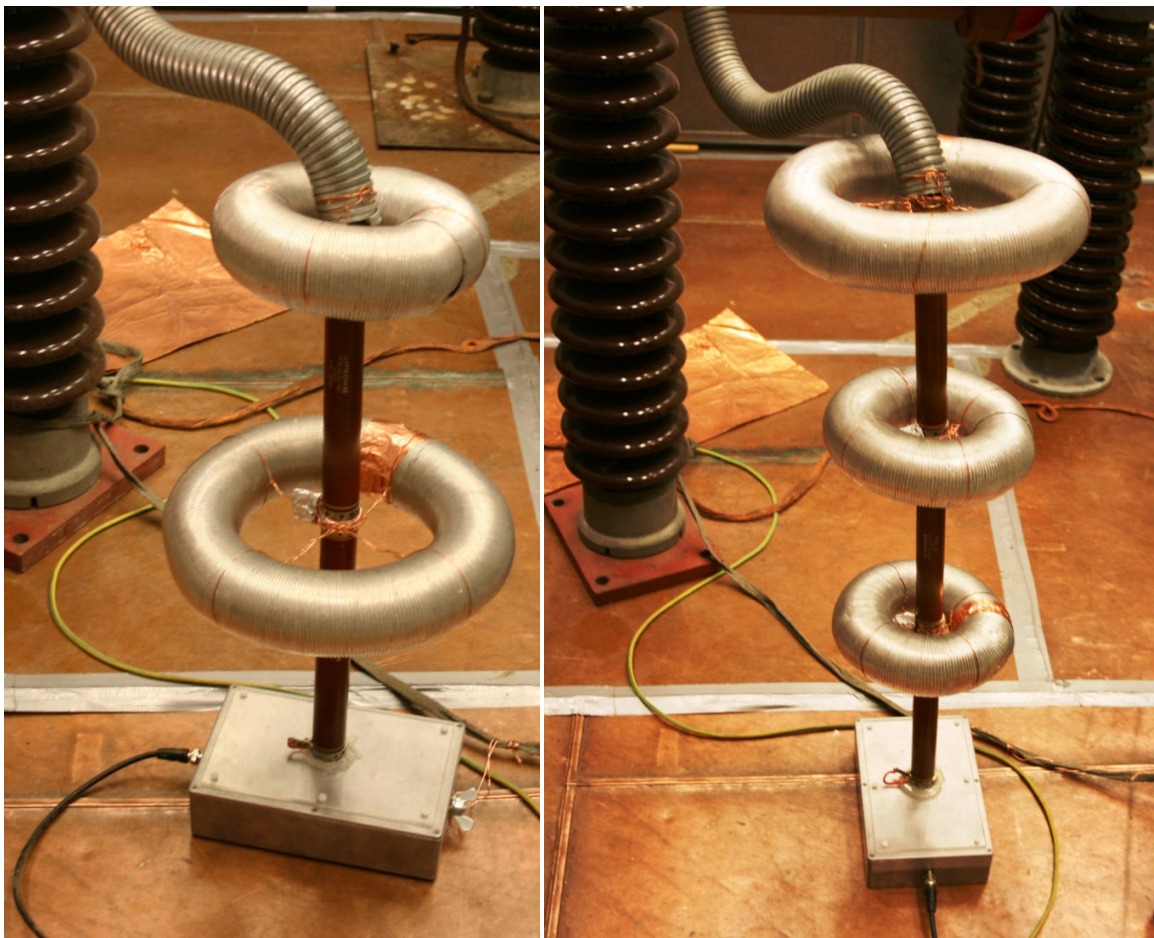


Figure 4.9 Left: The second voltage divider. Right: The third voltage divider.

4.2.1.2 Capacitive Voltage Divider

The capacitive voltage divider was chosen since the first resistive voltage divider built had too high amplitude of partial discharges, especially in the middle part of the divider, an effect due to a mistake in the construction. In general, partial discharges add to losses and the accuracy of the measured voltage may be reduced. This situation resulted in a voltage signal hardly differentiable from partial discharges and so a capacitive voltage divider was chosen instead.

The divider consisted of three capacitors; one standard capacitor of 100.19 pF in series with two parallel connected capacitors. A 1 μF with 10% capacitance tolerance and a 330 nF capacitor with 5 % capacitance tolerance. The voltage input to LabVIEW was measured across the parallel connected capacitors of 1.33 μF . This voltage divider gave a resolution of 2.0 V in the voltage measurement. No spark gap was used though the zener diodes were still connected at BNC adapter. The electric schematic of the capacitive voltage divider, without the zener diodes, can be seen in Figure 4.10.

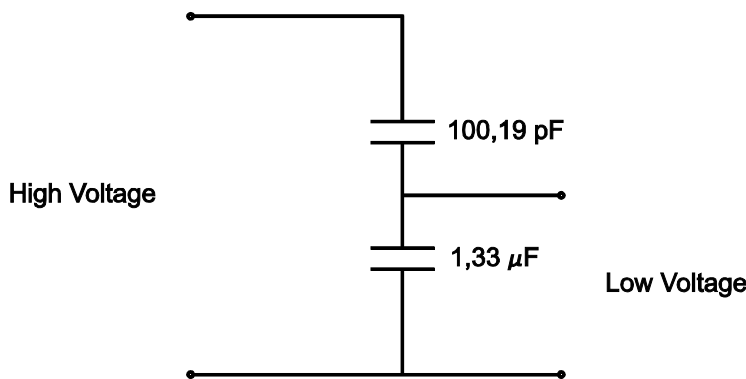


Figure 4.10 Schematic of the capacitive voltage divider.

4.2.2 Voltage Source

The “Phenix Technologies 600D series AC dielectric test set”, consisting of high voltage transformer, voltage regulator and control module, was used as the voltage source. The transformer has an output rating of 20 kVA, 75 kV and 0.267 A.

4.2.3 Capacitors

The smoothing capacitors, ASEA CHGA 51, used in the half-wave rectifier are “faradol impregnated all film” capacitors. They are 0.44 μF each and are rated for 120 kV DC voltage.

4.3 Transformer Oil

In order to prevent flashover across the test object, it was placed in an aquarium containing transformer oil. When a complete breakdown took place in the test object part of the semiconducting tab disintegrated and mixed with the oil. This coloured the oil black, diminishing its transparency. The soiled oil was filtered with the help of a büchner funnel

with paper filter and a büchner flask, to increase the visibility again. This procedure was done when possible depending of the blackness of the oil.

4.4 Signal Processing

The treeing videos and the voltage measurements were recorded on a computer for the analyses made after the testing was done. The low voltage signal from the voltage divider was connected to a National Instruments BNC 2110 adapter through a coaxial cable. Then the signal was further transmitted to a computer and a National Instruments DAQ S series 6143 data acquisition device.

4.4.1 LabVIEW Coordination with CCD Camera

National Instruments LabVIEW 8.6 was used to record voltage measurement during tests. A program saving the measured voltage and writing it into a text file in a loop structure was made. The block diagram of this program can be seen in Figure 4.11. The voltage was collected with a sampling frequency of 1000 Hz and ranged between -5 V and 5 V.

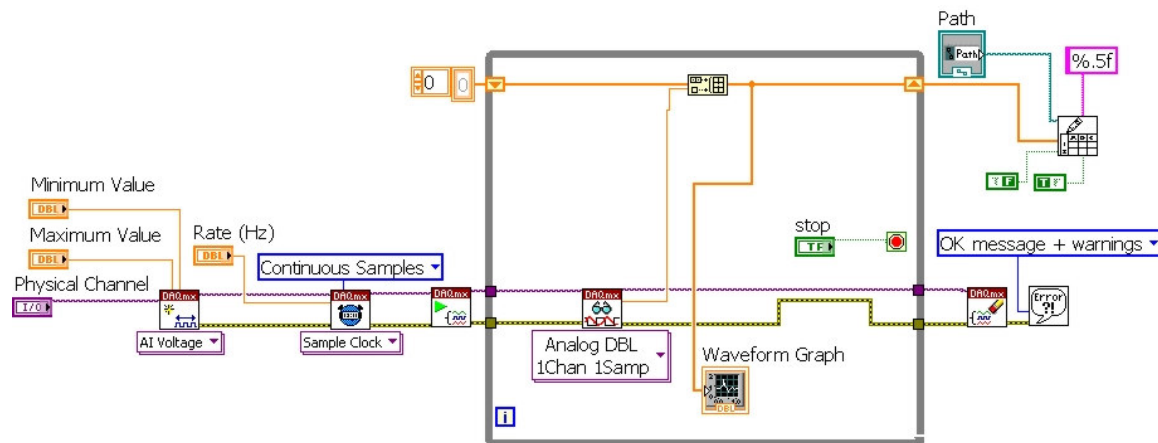


Figure 4.11 Block diagram of program used in LabVIEW to measure voltage.

The photos taken were recorded through Pinnacle video capture hardware in Pinnacle Studio 14. This treeing video had to be correlated to the voltage measurements; this was done manually as both were started individually from the computer screen. The recording clock in Studio was used as reference and when the video recording had been ongoing for 10 seconds the voltage measurement in LabVIEW was started. The error introduced by this procedure was evaluated in the DC measurements where the breakdown in the voltage measurement could easily be correlated to the breakdown captured in the video. The correlation error was checked for 29 available test results and it was found that that the voltage measurements were switched on between 0.2 s and 0.7 s too late. When comparing this error is much larger than the time error of 0.001 s in the voltage measurement, due to the sampling frequency and the time error introduced by the CCD camera of 0.04 s.

4.5 Voltage Determination

The behaviour of the AC and DC voltage applied to the test object is illustrated. How the measured voltage is converted to relevant data is described and assumptions are specified.

Two linear ramping functions available by the regulator were used, for both AC and DC stresses. Though, AC is referred to by its rms value since this is the mean voltage exposure, while DC in itself is a mean value. Also, active power is proportional to the rms value of the AC voltage and to the amplitude of the DC voltage, which gives an indication of the energy injected in the polymer.

4.5.1 AC Voltage Determination

This part describes assumptions taken regarding AC voltage measurement and how treeing initiation was determined for test object stressed with AC.

4.5.1.1 Assumptions

To specify at which voltage level the electrical trees are initiated the following assumptions were necessary to make:

- The measuring program in LabVIEW was started at exactly 10.000 seconds after the camera had begun capturing pictures.
- The AC voltage signal was symmetric around the offset value and the tree inception voltage could thereby be related to the positive values of the AC voltage signal.
- The measuring sampling frequency of 1000 Hz in LabVIEW provided an adequate sinus voltage wave form.

4.5.1.2 AC Voltage Measurement

The tree inception voltage level correlates to the time when the first electrical tree could be seen visually in the CCD camera video. For precise determination of tree inception there were some visual limitations, such as floating particles and electro hydrodynamic movements in the transformer oil. Since the contrasts and focus of the camera was not always perfect an oil movement could darken the pixels, indicating a false tree inception. Therefore the time for tree initiation was chosen when it could be confirmed from one picture frame to the next that the change was only due to treeing and nothing else. The picture analysis was done after the experiment had been performed.

The left hand pictures in Figures 4.12 and 4.13 display the measured voltage for the two ramping rates investigated, plotted in Matlab. The marker tips seen in the figures specify; the offset voltage value, the voltage level when the automatic ramping function was turned on and the peak voltage at the time for treeing inception. The offset voltage could differ at each test due to the floating ground potential of the measuring card and was corrected for, see Formula 4.1. The voltage level at the start of the ramp was also included in the formula. In Figure 4.12 two treeing inception voltages are specified; the lower corresponds to a tree at a kink and the higher one to a tree originating from the wire. For the test shown in Figure 4.13 no tree appeared at a kink.

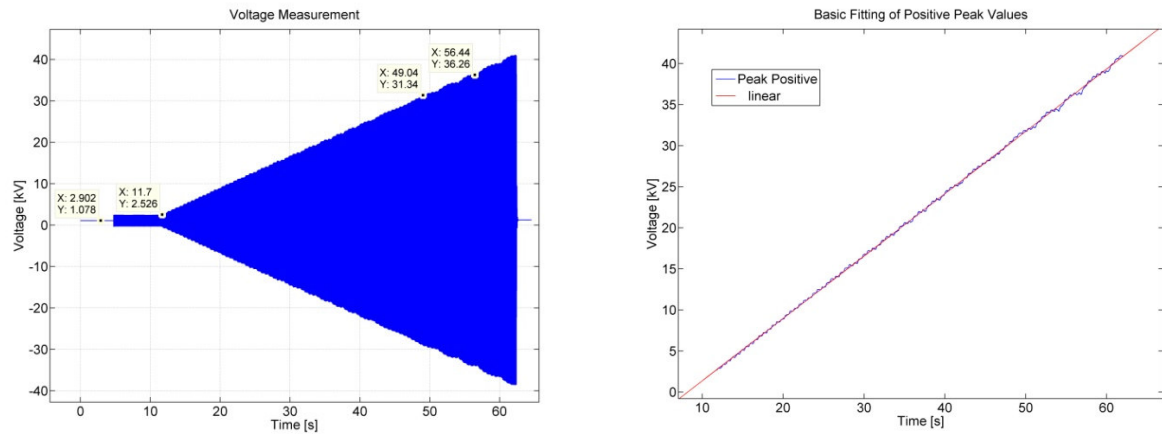


Figure 4.12 Left: Voltage measurement in LabVIEW for applied AC with a ramping rate of 0.5 kV/s. Right: Linear fit of the ramping for an AC voltage signal with a ramping rate of 0.5 kV/s. These measurements were made with a capacitive voltage divider.

The lower ramping rate of 0.5 kV/s is an arithmetic mean of the obtained ramping rates from Matlab applying linear fitting, the values span from 0.53 kV/s to 0.54 kV/s. See the right hand plot of Figure 4.12 for the ramping. Also 3.9 kV/s is an arithmetic mean in the same manner, with values between 3.82 kV/s and 3.89 kV/s.

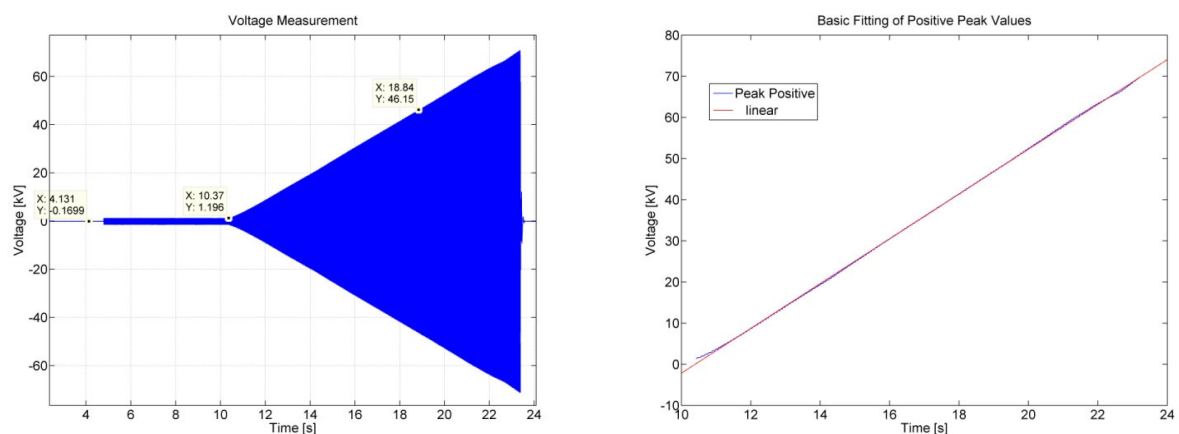


Figure 4.13 Left: Voltage measurement in LabVIEW for the applied AC with a ramping rate of 3.9 kV/s. Right: Linear fit of the ramping for an AC voltage signal with a ramping rate of 3.9 kV/s. These measurements were made with the third resistive voltage divider.

When comparing the linear fitting of the ramping it looks like the ripple is larger for the lower ramping rate than for the higher rate. This is due to the voltage axis; the absolute difference was small. The maximum deviation from the linear fitting plot, calculated by Matlab, to a voltage peak is 0.8 kV for the slower speed and 0.65 kV for the faster speed. Because of this ripple the linear fitting function was introduced. It includes more measurement points thereby reducing the error due to the added ripple.

The treeing inception voltage, $U_{inception}$, was determined by Formula 4.1:

$$U_{inception} = \Delta t * \text{ramp} + U_{ramp} - U_{offset} \quad (4.1)$$

where Δt is the time interval between the ramp start and the tree initiation, “ramp” is the ramping rate determined by the linear fitting function in Matlab, U_{ramp} is the voltage level at the start of the ramp and U_{offset} is the offset voltage.

The evaluation of the AC voltage signal showed that the sinus wave was slightly shifted around the offset level, in other words it is not perfectly symmetric around the offset level. The positive flank was 0.05 kV too low for the slower speed and 0.03 kV too low for the faster speed. This was not corrected for in the displayed results.

As is seen in Figure 4.14 the sampling frequency of 1000 Hz can cut of the peak of the voltage. The maximum error due to this was evaluated to 0.45 kV by superimposing a sinus wave on a signal missing the peak value. The error caused by the chosen sampling frequency was reduced by the use of the linear fitting function, mentioned before, since not all peaks were lost.

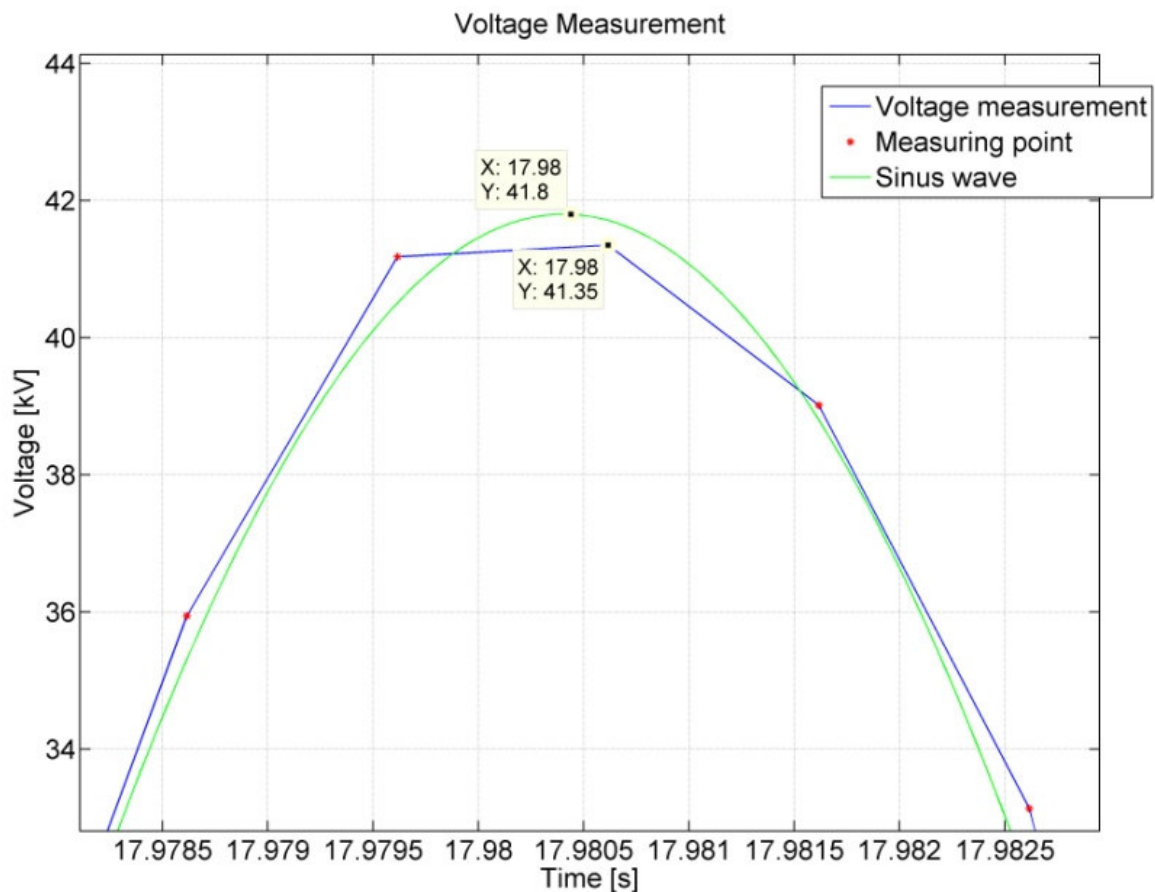


Figure 4.14 Close-up of voltage peak measurement together with a sine wave.

4.5.2 DC Voltage Determination

In the DC measurements the treeing initiation could not be seen with the CCD camera, see Chapter 5.2.1.1, instead the breakdown voltage, clearly visible in the voltage plot was measured. This was done visually by plotting the voltage measurements in Matlab. The value is then read directly in the graph without doing any linear fitting.

4.5.2.1 Assumptions

The following assumptions from the AC voltage determination:

The measuring program in LabVIEW was started at exactly 10.0 seconds after the camera had begun capturing pictures.

The measuring sampling frequency of 1000 Hz in LabVIEW is adequate for representing the voltage level shape.

4.5.2.2 Ramping Speed of 5.3 kV/s and -5.4 kV/s

The voltage across the test object can be seen in Figure 4.15. The very steep voltage drop was due to breakdown of the insulation and the residual voltage left at the test object was later removed by grounding the circuit. The ramping speed was calculated for all tests and for positive voltage polarity it varied between 5.25 kV/s and 5.34 kV/s, with an arithmetic mean of 5.3 kV/s. For the negative DC voltage the ramp speed varied between -5.39 kV/s and -5.46 kV/s, with an arithmetic mean of -5.4 kV/s. The asymmetric AC voltage might be the source of this discrepancy.

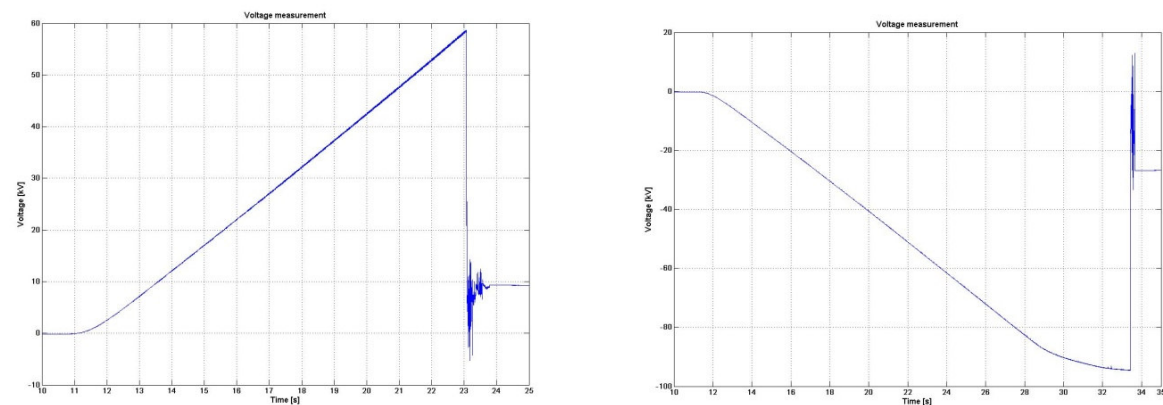


Figure 4.15 Left: The voltage at the test object at test with positive DC voltage polarity. Right: The negative DC voltage at the test object.

The voltage ramp was rather smooth with the AC ripple being less than 0.6 % of the applied voltage. After the voltage drop the voltage oscillated during approximately 0.5 seconds before it stabilised again. The peak-to-peak values of these oscillations were at the most 60 kV, although this magnitude varied in different tests. It is worth noticing that electrical trees were initiated at voltage levels spanning from 22 kV (rms) in the AC tests, see Chapter 5.1.3. Negative polarity of the applied voltage required a higher voltage level for breakdown of the test object, thus the ramp became unlinear as it flattened out at the maximum voltage level of approximately 100 kV. Figure 4.16 shows the ripple in the ramp for the positive polarity at the level of 55.5 kV.

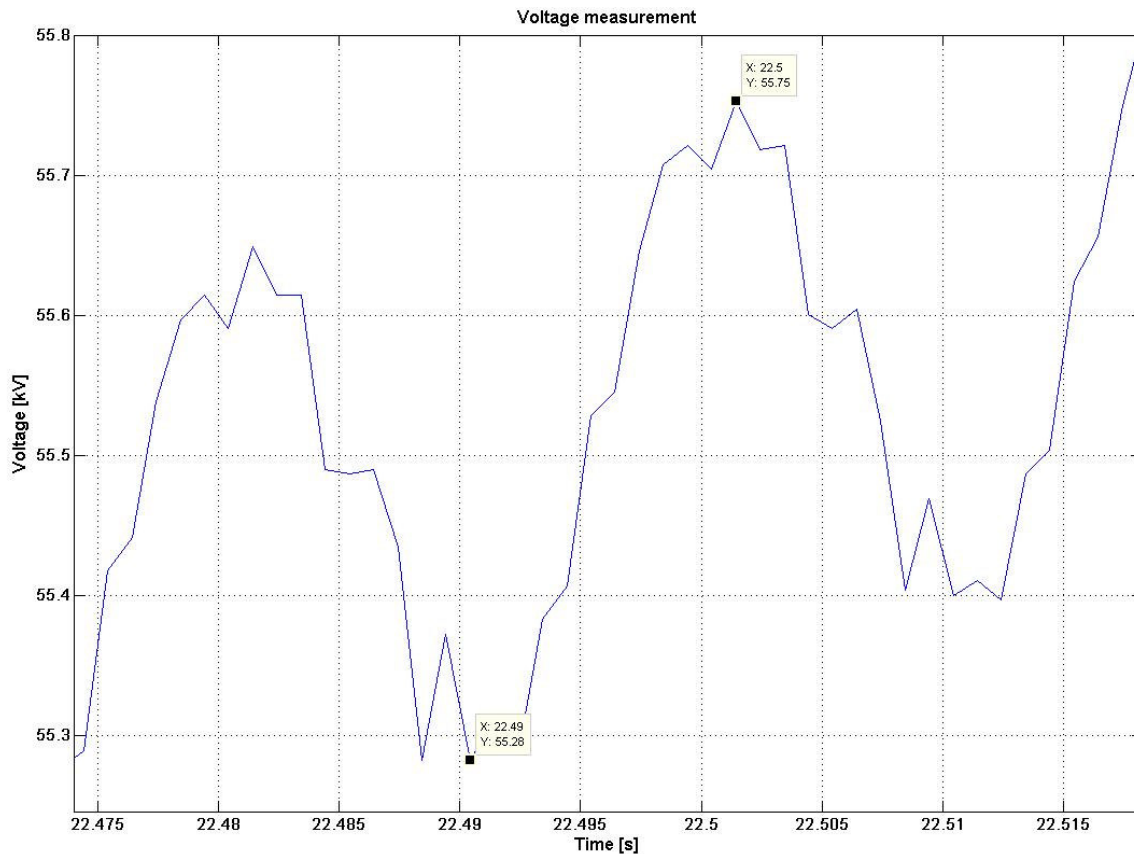


Figure 4.16 Close up of the ripple superimposed on the DC voltage ramp.

4.5.2.3 Ramping Speed of 0.7 kV/s and -0.7 kV/s

With a few exceptions the voltage behaviour was similar for the slower ramp speed. The ramping speed was calculated to 0.7 kV/s and -0.7 kV/s respectively and the ripple was slightly higher, less than 1.5 % of the applied voltage.

The second resistive voltage divider broke down evaluating this ramp speed and was replaced by the third resistive voltage divider.

4.6 Weibull Analysis

The collected data were analysed and probability plots were made using the software Minitab 15. This software uses least squares regression to estimate the parameters of the two- and three-parameter Weibull distribution. The two parameter distribution was chosen when the requirements of the three-parameter Weibull distribution were not fulfilled [7].

5 Results

This chapter describes achieved results and comparisons of AC inception voltages with previous work, different ramping rates, treeing at kink and at wire, breakdown voltages for positive and negative polarity and AC compared with DC. The effect of varying temperature in the transformer oil is also covered.

5.1 Electrical Treeing Due to AC Stress

Two examples of how the test objects look in a microscope after they have been stressed by AC voltage can be seen in Figure 5.1. The amount of electrical trees developed has varied from 1 tree up to 21 trees for a single test object. The treeing structures found are bush, branch, bush-branch, mirror-trees and mini-trees, examples of these tree shapes were shown in Figure 2.1. There was though an excess of dense formations. The lines that seem to go randomly in the figure are scratches on the surface of the test object. In the left picture the grounding plane can be seen with silver paint on, the greyish part at the top.



Figure 5.1 Two examples of AC test objects (0.5 kV/s) showing varying amounts of electrical trees.

The silver paint was observed to fall off during the first tests carried out with the AC voltage source operated at the ramping rate of 0.5 kV/s. Flakes were floating around in the transformer oil. Since the silver was at floating potential it might have affected the electrical field and consequently influenced the treeing process. This was thought not to be the case, for further discussion see Chapter 6.3. For the test object just mentioned a breakdown occurred from the wire through the width of the sample to the surface. This was most likely due to a very large ($\approx 3\text{mm}$) flake localized in near vicinity to the surface, see Figure 5.2. To eliminate the element of uncertainty of the paint it was removed with isopropanol for further experiments, i.e. for the AC tests with a ramping speed of 3.9 kV/s and for the DC tests.

All ramping speeds and tree inception voltages in this chapter refers to rms values of AC voltage.

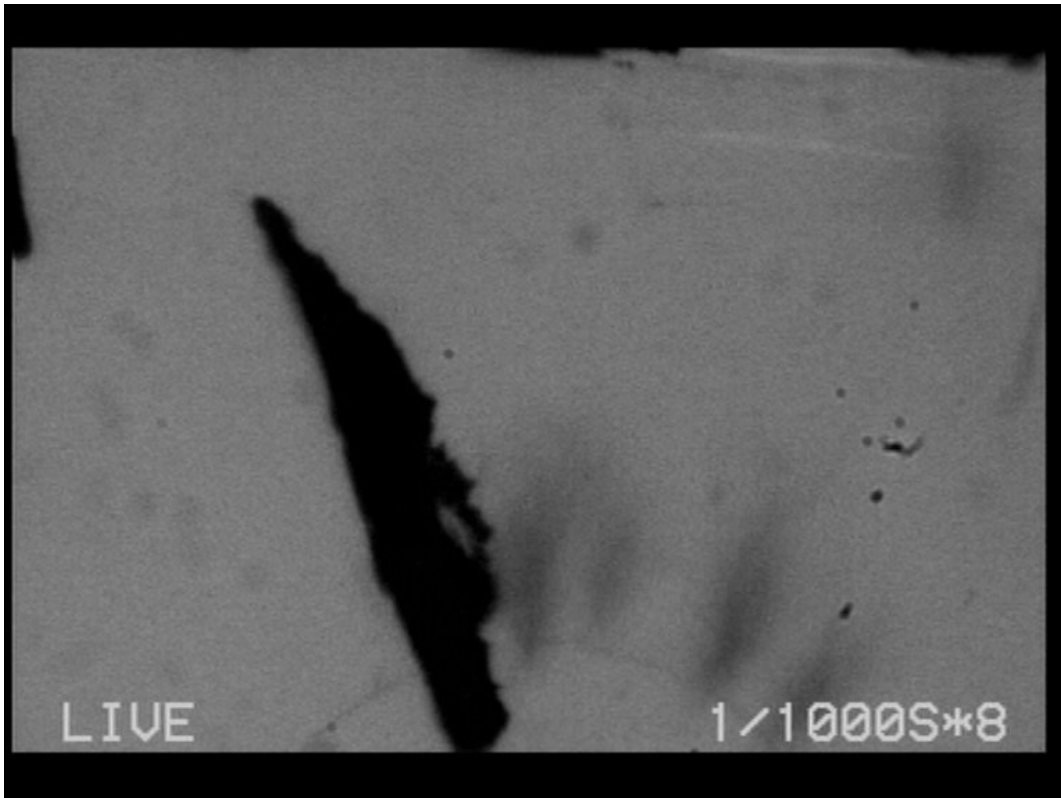


Figure 5.2 Picture capturing a large flake of silver paint that was most likely the cause of a breakdown through the width of one test object.

5.1.1 Comparison with Previous Work

For the previous work with the same electrode configuration, [7], [27], an AC voltage source was used with a ramping rate of 0.5 kV/s to test an XLPE insulation material. These results were compared with the AC results achieved in this project where the same ramping rate was used. The insulation materials are both XLPE but crosslinking level, type of additives and the amount of crosslinking byproducts are likely to differ.

The tree inception voltage was converted to treeing initiation field by Formula 5.1:

$$E_{rms} = K \cdot U_{rms} \quad (5.1)$$

where E_{rms} [kV/mm] is the electric field strength at the wire surface, U_{rms} [kV] is the applied voltage of the test object and K [mm^{-1}] is equal to 19.5, which corresponds to a conducting wire with a diameter of 10 μm . This relation and the value of constant K was found by linear regression originating from the previous work [7], [27], where the electrode configuration was modelled in Comsol Multiphysics Package[21].

The comparison was made with the 3-parametric Weibull probability plot with a 90 % confidence interval, see Table 5.1. It can be seen that the treeing initiation fields for “XLPE [7]” are less spread in field strength amplitude than “XLPE used in test” due to a higher value of the shape parameter. The failure probability of 63.2%, represented by the scale, also requires a higher electric field for the XLPE used in previous work [7] whilst the threshold of the initiation field is higher for the XLPE used in this project.

Table 5.1 Comparison of Weibull distribution parameters with previous work [B] for AC 0.5 kV/s. Voltages are given as rms values.

Material	Shape, α	Scale, β [kV/mm]	Threshold, γ [kV/mm]	# samples
XLPE used in test	1.7	105	420	19
XLPE [B]	2.4	206	365	45

The tree initiation field values ranged from 400 kV/mm to approximately 700 kV/mm for the previous work [7]. In this project they have a comparable range with values between 430 kV/mm and 660 kV/mm.

5.1.2 Comparison of AC Tree Inception Voltages with Different Ramping Rates

The two experiments made with applied AC voltage differ in two ways. First, the lower ramping rate of 0.5 kV/s was performed with test objects having a grounding plane covered with silver paint while it was removed for the test objects stressed with the faster ramping rate of 3.9 kV/s. The silver paint was considered not to influence the tree inception voltage. Secondly, the voltage was measured with a capacitive voltage divider for tests made with 0.5 kV/s and respectively with the third resistive voltage divider when 3.9 kV/s was used. The comparison was made with the 3-parametric Weibull probability plot with a 90 % confidence interval, see Figure 5.3. All the inception voltages refer to the first tree that originates from the surface of the conducting wire, thus a tree initiated at a kink is excluded.

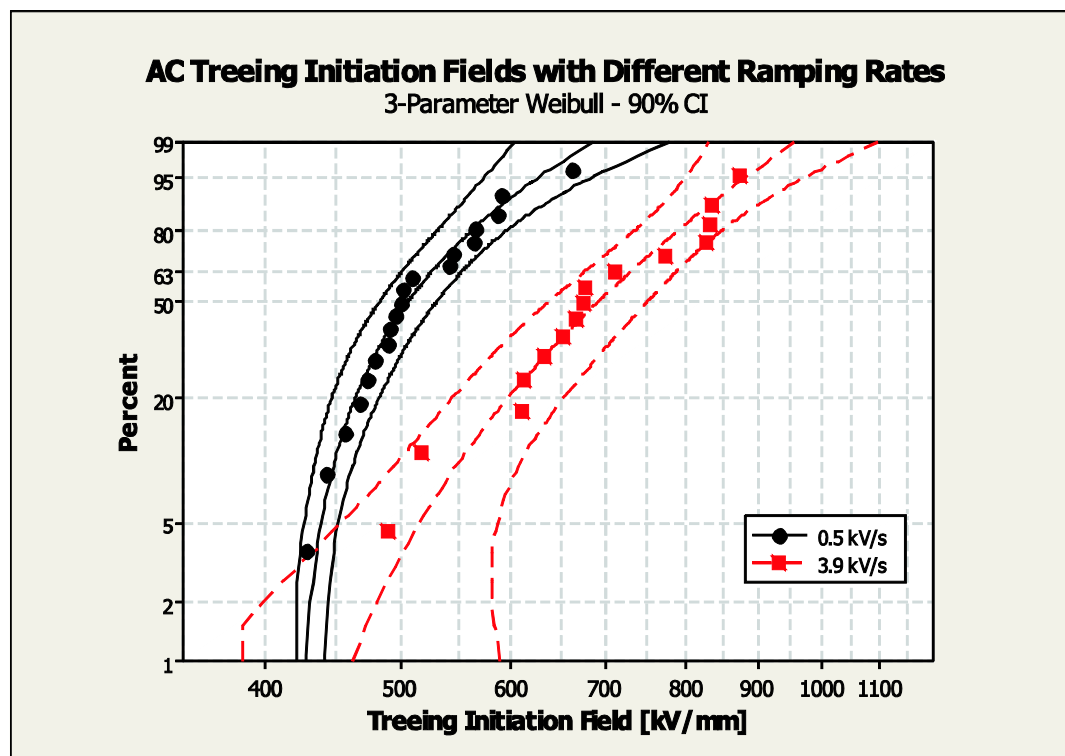


Figure 5.3 Comparison of 3-parametric Weibull probability plots of AC treeing initiation fields with 0.5 kV/s and 3.9 kV/s ramping rates.

It can be seen from Figure 5.3 that a higher ramping rate results in a higher treeing initiation field. For the ramping rate of 0.5 kV/s treeing initiation field ranges between 430 kV/mm and 660 kV/mm, as mentioned in Chapter 5.1.1, and for 3.9 kV/s it spans from 490 kV/mm to 870 kV/mm. The Weibull distribution parameters are specified in Table 5.2. The threshold parameters imply that failure will be noticed earlier for the higher ramping speed though this was not the case in practise. It might be due to the 90 % confidence interval and to the two lowest outlying values of the 3.9 kV/s ramping rate. The higher parameter values of shape and scale for the faster ramp rate indicate what can be seen in Figure 5.3, treeing initiation voltages are more spread, i.e. has a slower ageing process, than for the lower rate.

Table 5.2 Comparison of Weibull distribution parameters of AC treeing initiation fields with 0.5 kV/s and 3.9 kV/s ramping rates.

Ramp rate	Shape, α	Scale, β [kV/mm]	Threshold, γ [kV/mm]	# samples
0.5 kV/s	1.7	105	420	19
3.9 kV/s	3.1	344	385	15

Different ramping speeds also affected the tree growth rate; 3.9 kV/s gave a more accelerated treeing development than 0.5 kV/s. The progression is visualized for the two ramping rates in Figure 5.4 and Figure 5.5. In Figure 5.4 the three first pictures are separated in time with 4 seconds while the last picture shows the final amount of trees when the voltage source was turned off, 10 seconds after the third picture. Figure 5.5 has a similar treeing development except for the time difference; these pictures were captured only 1 second after each other.

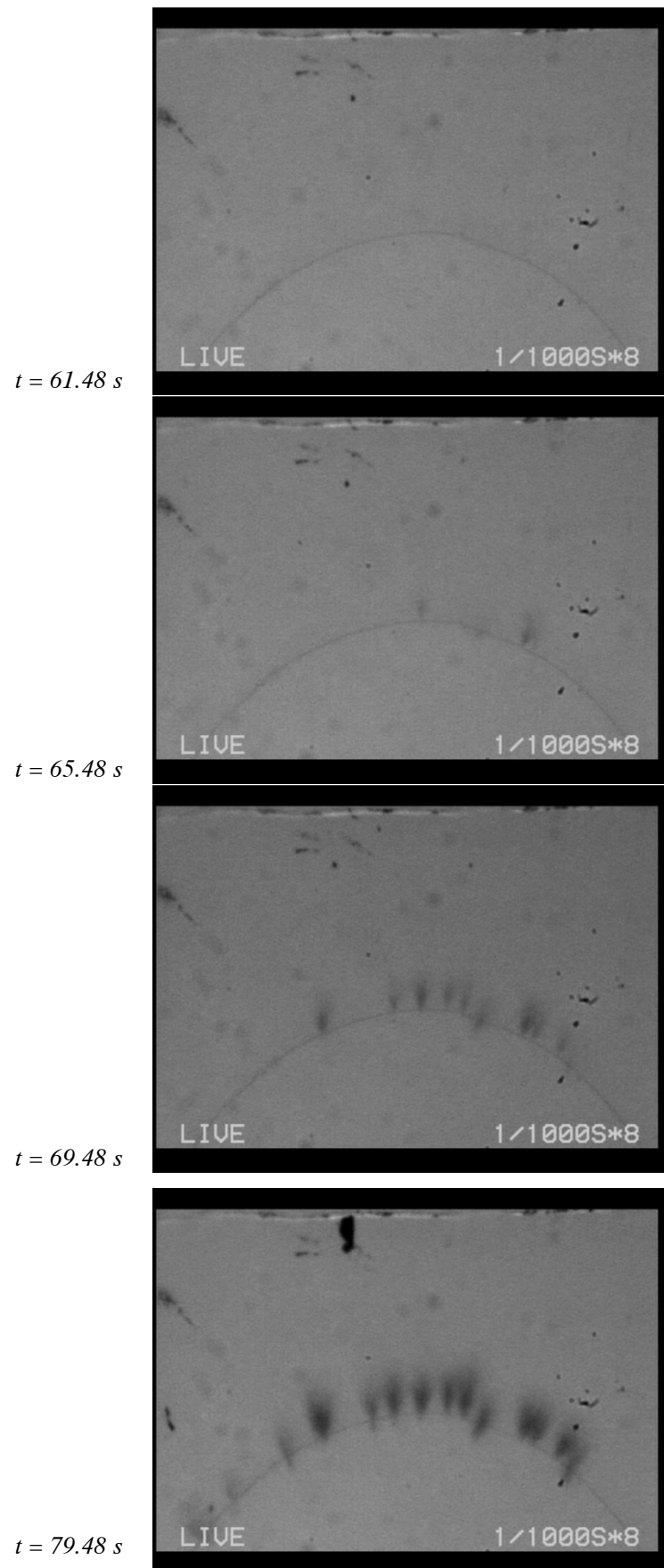
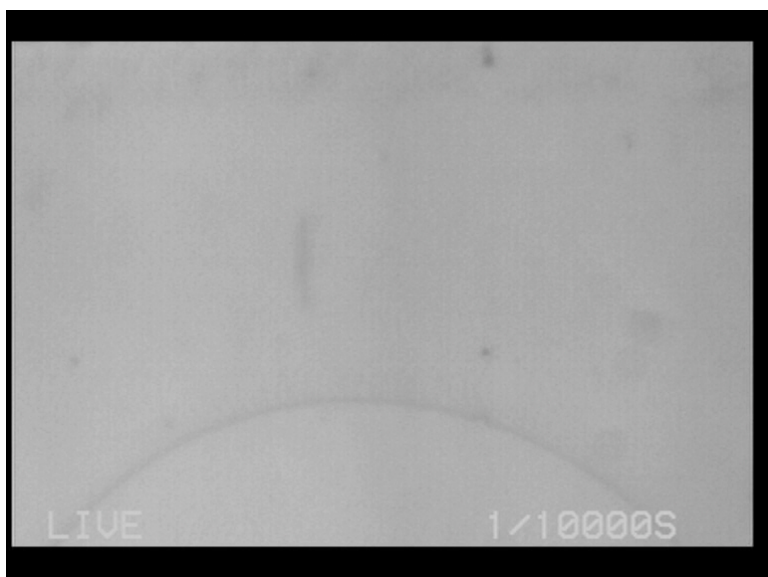
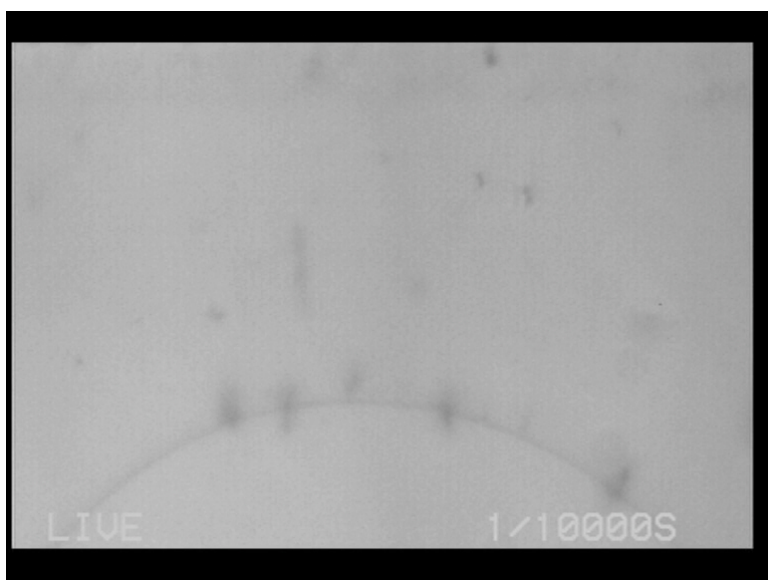


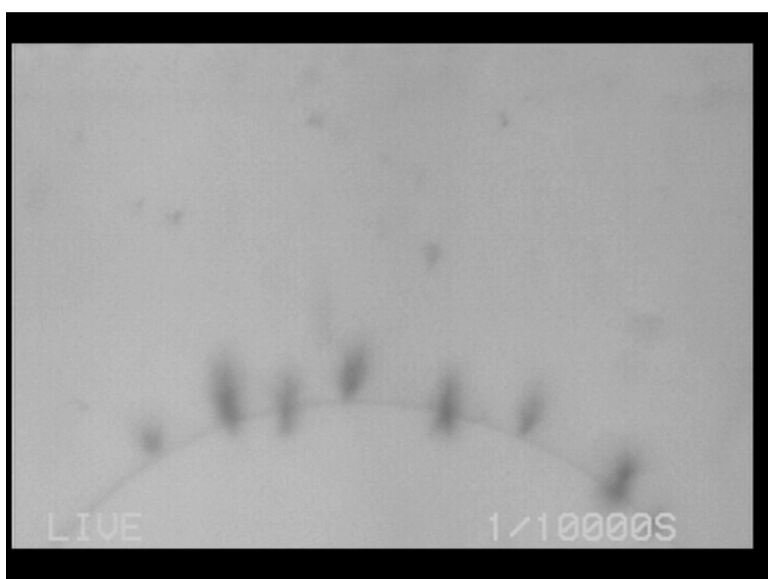
Figure 5.4 *Tree developments for insulation exposed to 0.5 kV/s AC stress.*



$t = 28.48 \text{ s}$



$t = 29.48 \text{ s}$



$t = 30.48 \text{ s}$

Figure 5.5 *Tree developments for insulation exposed to 3.9 kV/s AC stress.*

5.1.3 Comparison of Tree Inception Voltages for Treeing at Wire vs. Treeing at Kinks

Comparison of tree inception voltages for treeing at wire with treeing originating at kinks with a 3-parametric Weibull probability plot could only be made for AC with a ramping rate of 0.5 kV/s, see Figure 5.6. This due to only two samples found with trees at kinks for the tests made with the other ramping speed of 3.9 kV/s. This is not considered as enough data to draw conclusions from. The comparison was done with inception voltages instead of initiation fields since the relation of Formula 5.1 in Chapter 5.1.1 refers to the geometry of a conducting wire and not to the formation of a kink.

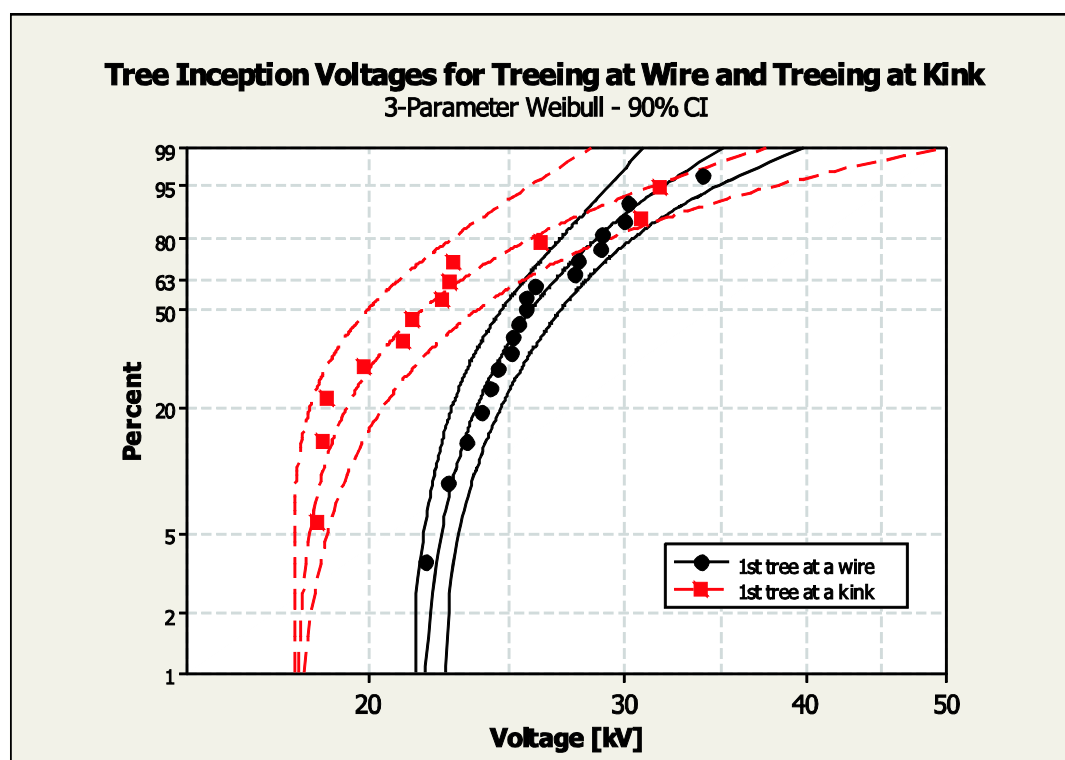


Figure 5.6 Comparison of tree inception voltages for normal treeing and treeing by kinks with 3-parametric Weibull distribution plot. Both plots with an applied AC voltage with a ramping rate of 0.5 kV/s.

It can be seen from Figure 5.6 that treeing inception voltages at kinks are lower in amplitude than treeing developed from the wire surface. Two separate distributions are apparent though they are not very distinct; the scale parameters are equal and the threshold values differ with 3.8 kV (i.e. 17.6 % referring to the threshold of treeing at wire), see Table 5.3. The treeing at kinks are though more spread in range which is also confirmed by the low shape parameter.

Table 5.3 Comparison of Weibull distribution parameters of inception voltages for treeing at wire vs. treeing at kink. Ramping speed for both results were 0.5 kV/s.

Treeing at	Shape, α	Scale, β [kV]	Threshold, γ [kV]	# samples
Wire	1.7	5.4	21.6	19
Kink	1.2	5.4	17.8	12

Treeing at kinks vary for the two ramping speeds used, statistics are shown in Table 5.4. The samples included in the statistics are the ones where kinks could be seen in the microscopic photographs. Specimens where a breakdown occurred are excluded. This adds up to 19 samples for the slower ramping speed and 10 samples for the faster. The kinks were only included if they were located on the upper half of the wire loop, as no trees could be found on the lower half closest to the semiconducting tab. For the slower ramping speed 12 out of 19 samples had the first tree at a kink, 63% of the total number of kinks had a tree and 37% had kinks without trees. Corresponding data for the faster speed where; 2 out of 10 samples with a first tree at a kink, 60% of the total number of kinks had a tree and 40% were without. The total number of kinks was 27 for the lower ramping rate and 15 for the faster.

The amount of kinks on the whole wire varied in a span from 1 to 5 per sample. Only one out of 29 of the test objects included in Table 5.3 was entirely without kinks.

Table 5.4 *Statistics of treeing at kinks on the upper half of the wire loop, the one closest to the grounding plane. Percentages of total number kinks are shown in parentheses.*

Ramping rate	Total # of samples	Total # of kinks	# 1 st tree at a kink	# kinks with tree	# kinks without tree
0.5 kV/s	19	27	12	17 (63%)	10 (37%)
3.9 kV/s	10	15	2	9 (60%)	6 (40%)

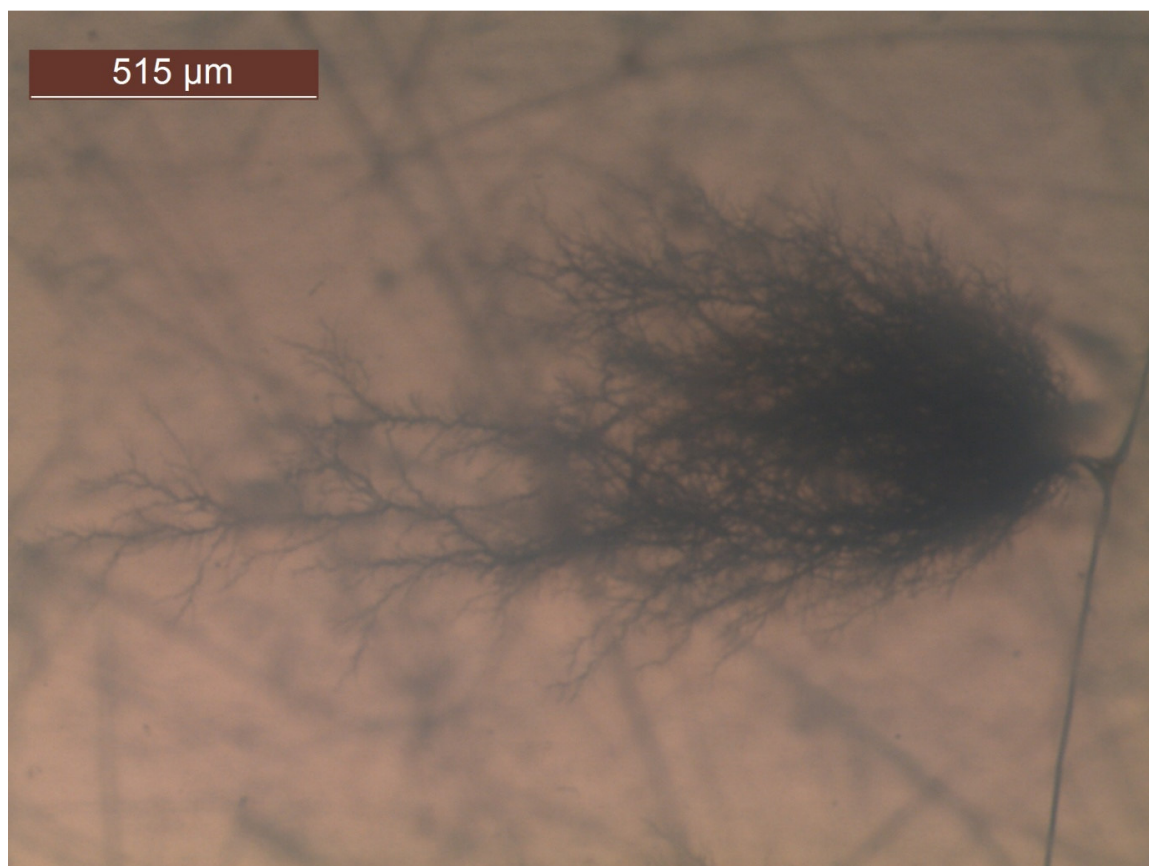


Figure 5.7 *Treeing at a kink, starting as a bush-tree and ends up as a bush-branch tree.*

5.1.4 Breakdown Channel Formation during Tests with Applied AC Voltage

A channel is formed due to a breakdown in the dielectric material. For the AC tests this occurred once for the ramping speed of 0.5 kV/s and for six test objects with the ramping speed of 3.9 kV/s. In Figure 5.8 test object can be seen stressed with the ramping rate of 3.9 kV/s. The electrical trees started to grow and finally a breakdown formed a channel from the wire at high voltage potential to the grounding plane. It is likely that the channel sprung from an already existing tree since parts of the branches are still distinguishable, see Figure 5.9. For this test object a smaller fraction of the wire close to the breakdown channel has been replaced by a thicker tube formation. In one AC case the whole wire was widened and for two samples the wire on one side of the breakdown channel became wider. All these cases refer to the faster ramping speed for which it was more difficult to switch off the voltage supply before the tree bridged the 3 mm separation of the electrodes and thus breaking down the XLPE.

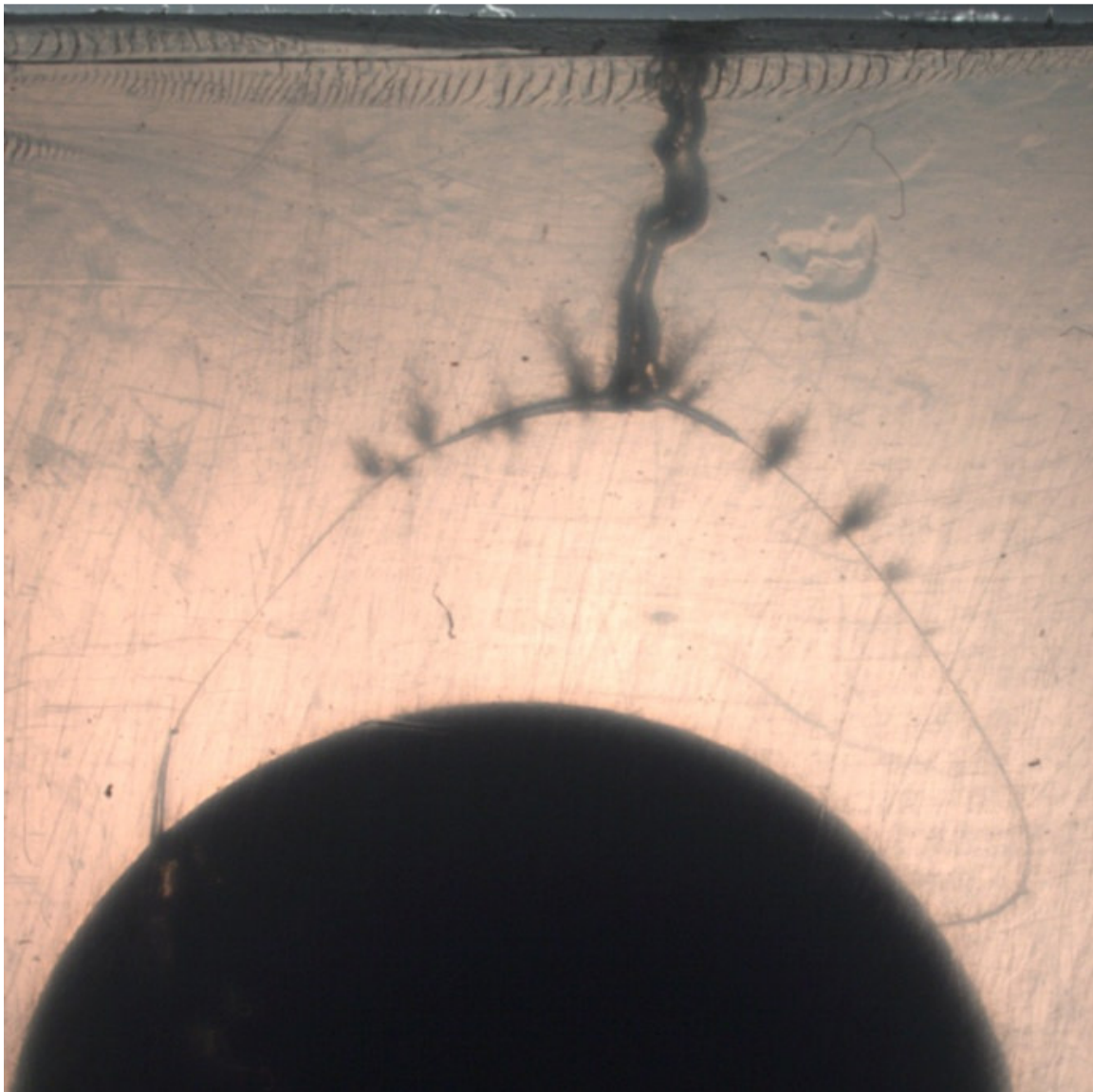


Figure 5.8 Test object stressed with AC voltage (3.9 kV/s) showing a breakdown to grounding plane.

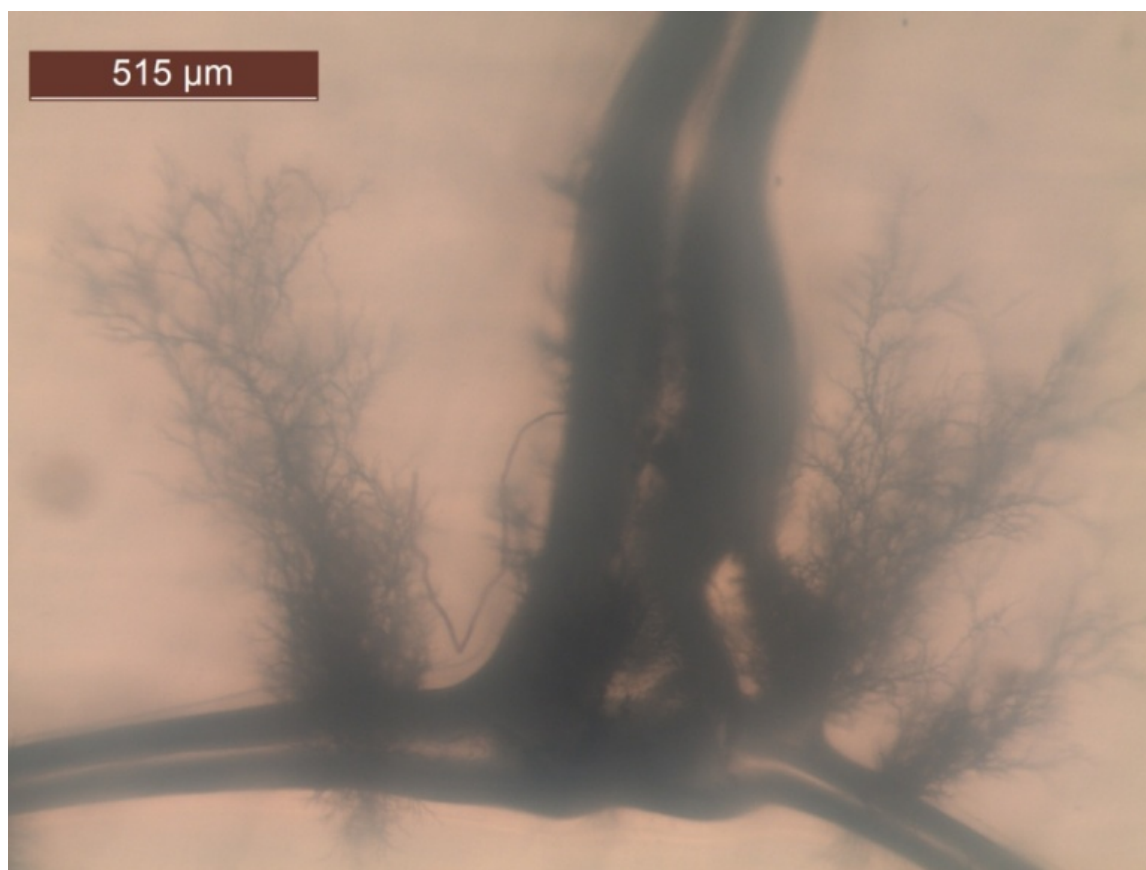


Figure 5.9 *Close up of the channel beginning from wire with surrounding trees.*

A view of another breakdown channel reaching the grounding plane can be seen in Figure 5.10. The channel has split in two and much thinner branches are noticeable originating at the channel. Also these are growing towards the grounding plane. A close up of the breakdown channel is shown in Figure 5.11,

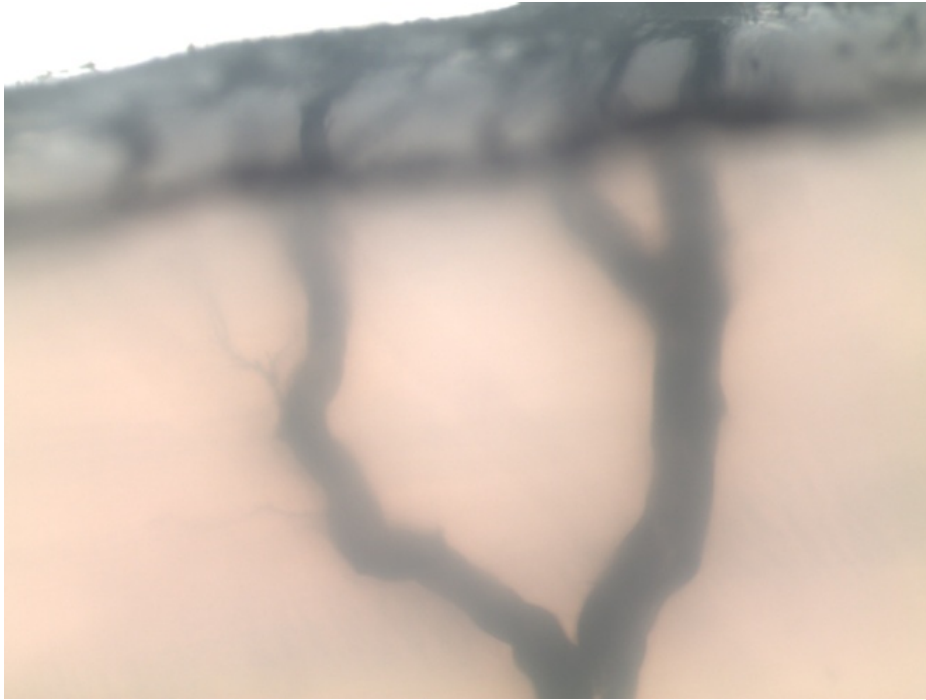


Figure 5.10 Test object stressed with AC voltage (3.9 kV/s) showing the end of the breakdown channel reaching the ground plane.



Figure 5.11 Close up of a breakdown channel for a test object stressed with AC voltage.

5.2 Electrical Treeing due to DC Stress

The main focus in this master thesis has been to detect and analyse electrical treeing phenomena at DC stress. For this purpose the circuit was adapted and the AC voltage was rectified. Different voltage ramping speeds were tested in order to find a suitable one, which would initiate treeing in the XLPE without causing a flashover somewhere else in

the circuit before that. The ramping rate of 3.9 kV/s (rms), corresponding to 5.3 and 5.4 kV/s for positive and negative polarity in the DC circuit, was found adequate and was used in the first series of breakdown tests. Later on also 0.5 kV/s (rms), corresponding to 0.7 kV/s, was attempted in order to compare with the AC results. The test objects used in the DC experiments had no silver paint. The air temperature was around 25 °C and the temperature of the oil surrounding the test object varied between 23 °C and 41 °C, due to heating by the lamp. The impact of the oil temperature is further discussed in Chapter 5.3.

5.2.1 Breakdown Tests at Ramping Speeds of 5.3, –5.4 kV/s

For the first ramping speed 10 test objects were stressed with a voltage of positive and negative polarity respectively. Some basic information on the statistics, concerning breakdown and tree structure of the tested samples, is compiled in Table 5.5. The AC voltage source was ramped up to the highest possible level 72 kV (rms), without triggering the overvoltage protection. This corresponds to 102 kV in the rectified DC voltage. After the testing was complete, all samples were checked, for details of the breakdown channel and for visible tree structure, in a microscope. Electrical trees were found in some samples, but the majority of the samples showed no sign of tree structures. By comparing the images from the CCD camera with the microscope images the position of kinks was checked and this made it possible to confirm whether the channel had formed at a kink or not. The breakdown was considered to originate from the kink if such was visible in the vicinity of the channel when comparing the two image types. For positive polarity six out of nine channels appear at or in the vicinity of a kink, for the remaining three it is unclear if there are kinks at the channel due to bad quality of the CCD camera images. For negative polarity four out of six samples have a confirmed kink at the breakdown channel and for two it is unclear. As a result to this fact, calculating the corresponding electric field is not applicable for the DC case. Thus the voltage level, applied to the semiconducting tab and wire, for which breakdown occurred is presented in the following results.

Table 5.5 *Sample statistics*

Polarity	# samples tested	# samples with visible tree structure	# samples with breakdown from the wire	# samples with confirmed channel at kink
Positive	10	4	9	6
Negative	10	3	6	4

5.2.1.1 Breakdown Characteristics

A difference from the AC method was the rapid behaviour preventing the voltage from being switched off before breakdown. Breakdown occurred even faster than could be recorded by the camera. The consecutive sequence of pictures seen in Figure 5.12 shows this fast breakdown. In the first frame the wire can be seen without any visible trees. The darker spots noticeable in this image are particles in the oil. The following frame, captured 0.04 seconds later, shows the breakdown taking place whereas 0.04 seconds later the picture is completely black. The pictures were not used in the measurements and the breakdown voltage is referred to, as opposed to the tree inception voltage and the tree initiation field used in AC analysis.

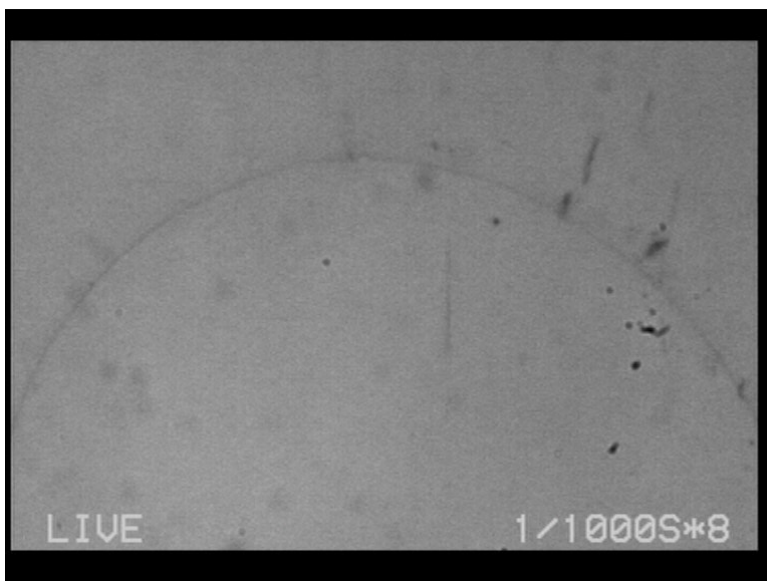
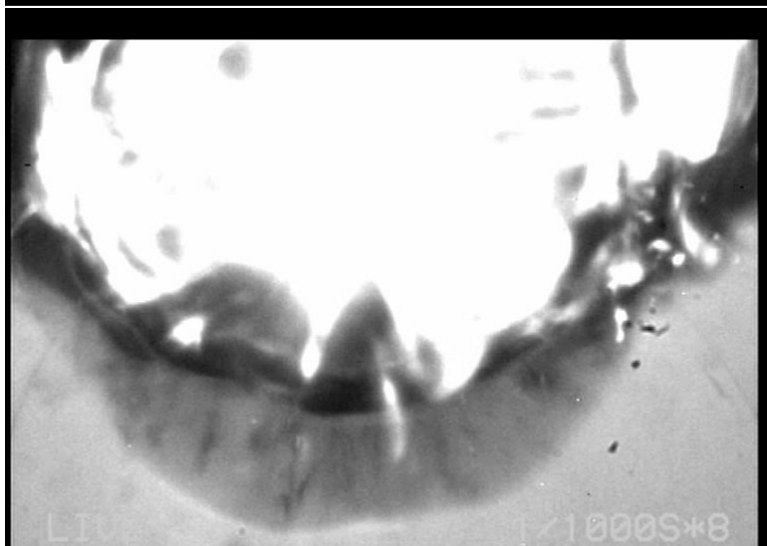
$t = 34.04 \text{ s}$  $t = 34.08 \text{ s}$  $t = 34.12 \text{ s}$ 

Figure5.12 Consecutive sequence of pictures. From the DC test with positive polarity and a ramping speed of 5.3 kV/s.

The XLPE broke down between the wire out to the oil on the side, instead of breaking down between the wire and the ground plate, as was expected. This breakdown happened either towards the glass wall of the aquarium or in to the oil on the other side and towards the grounding wire connected to the ground plate, with some tendency in breaking down towards the glass. An example of this behaviour is shown in Figure 5.13. This happened for all test objects used in the analysis, i.e. the ones where breakdown occurred in the XLPE before a flashover happened elsewhere in the circuit.

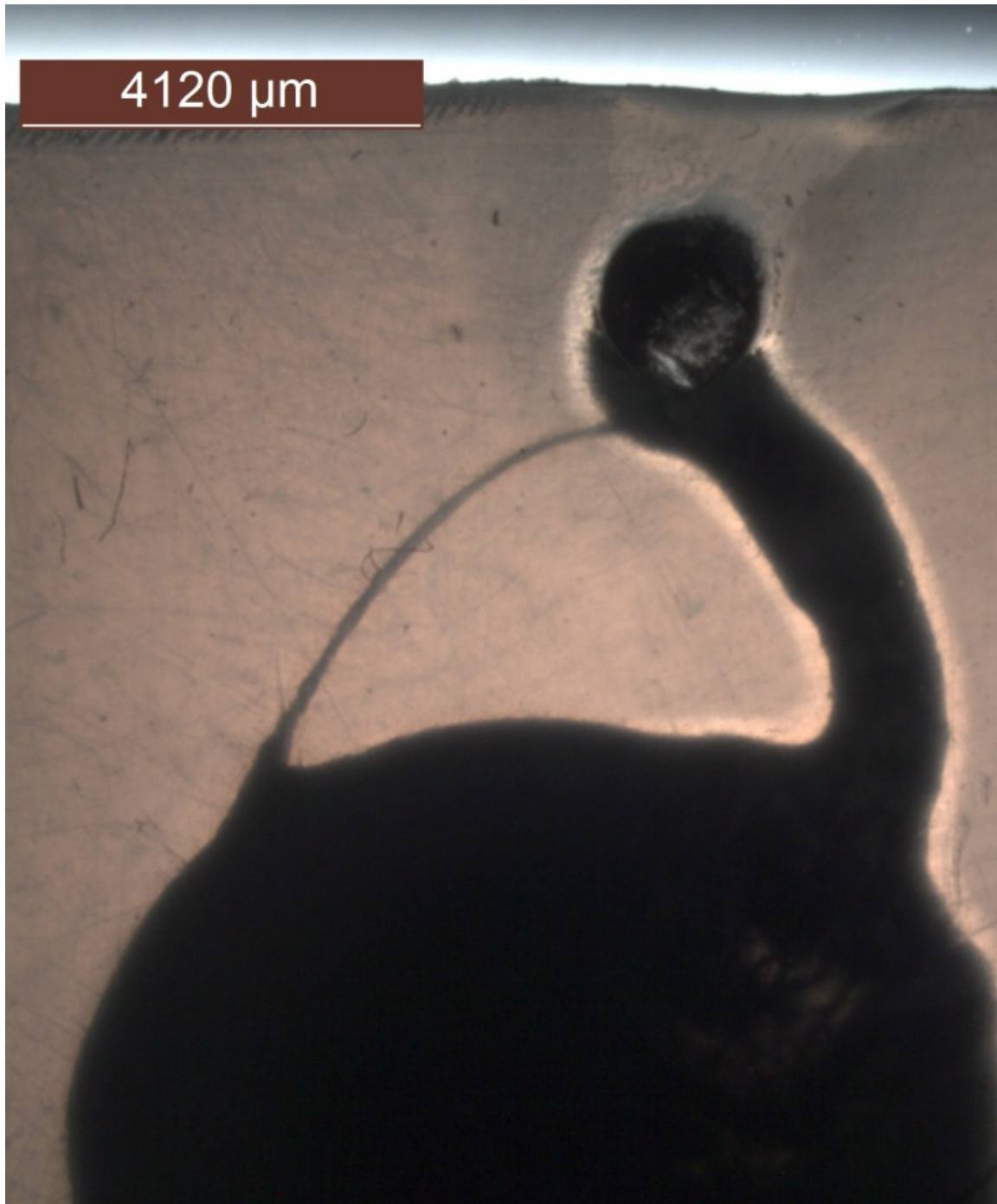


Figure 5.13 A distinctive breakdown channel, which has gone through the width of the test object and formed a wide tube around the wire on one side of the breakdown channel. Around the wire on the other side a smaller tube has been formed.

There are diverse cases of breakdown behaviour in the XLPE. For the first case a wide tube has been formed around the whole wire, shown in Figure 5.14, destroying any existing trees initiated by the voltage ramp.

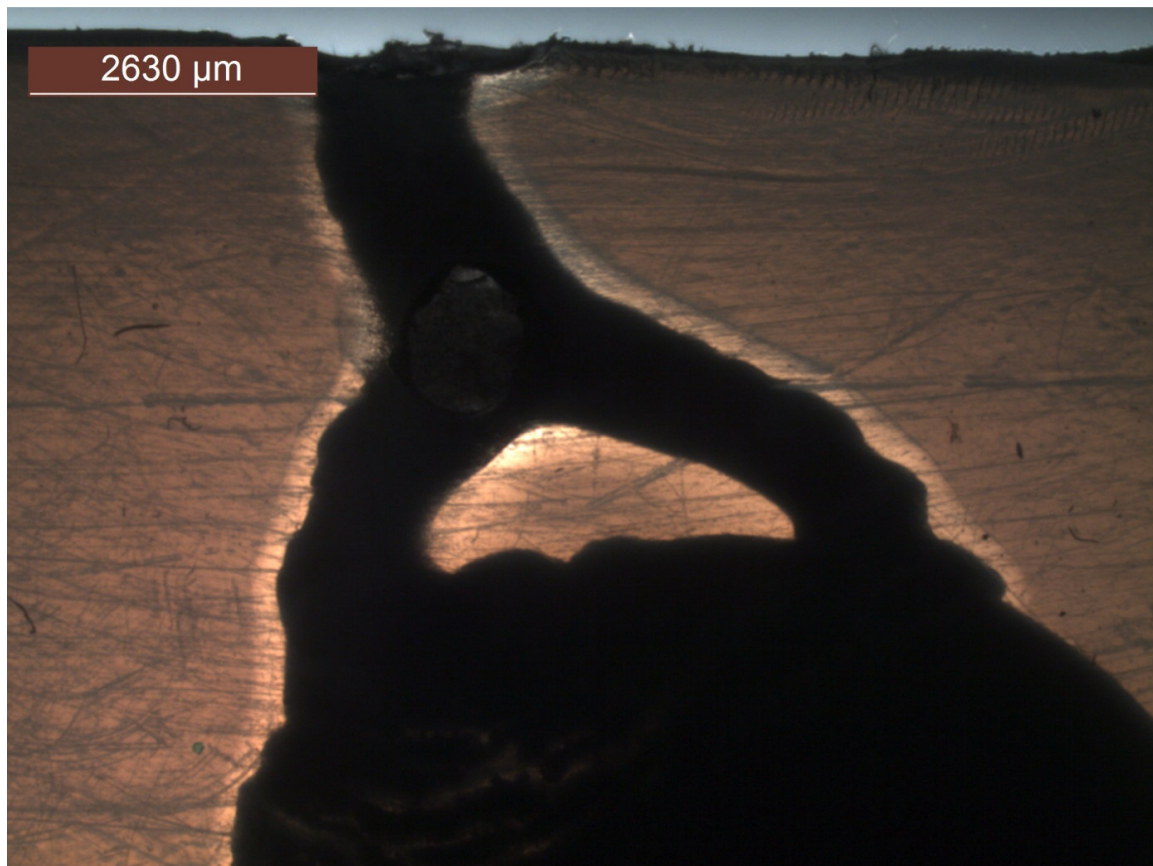


Figure 5.14 A large breakdown channel, the change in the surrounding XLPE is also visible. The breakdown has divided to form one channel going towards the viewer and one channel towards the ground plane in the top of the picture.

The second case, exhibited in the majority of the samples, has a wide tube formed along the wire on one side of the breakdown channel, see Figure 5.13. On the other side there is a narrower tube formed around the wire. This made it likelier to find remnants of trees there, as is the case for two of the test objects, where electrical trees have been spotted along this side of the wire. Examples of trees found along this side of the wire can be seen in Figure 5.15-5.17. These trees might have been present when breakdown took place or they might have been initiated by the breakdown itself. A hypothesis is that the thicker tree, shown in Figure 5.17, was affected by the formation of the tube around the wire while breakdown occurred, and thus was there before the breakdown, whilst the thinner trees in Figure 5.15 and Figure 5.16 were initiated or began growing at the breakdown or possibly by the oscillating voltage.

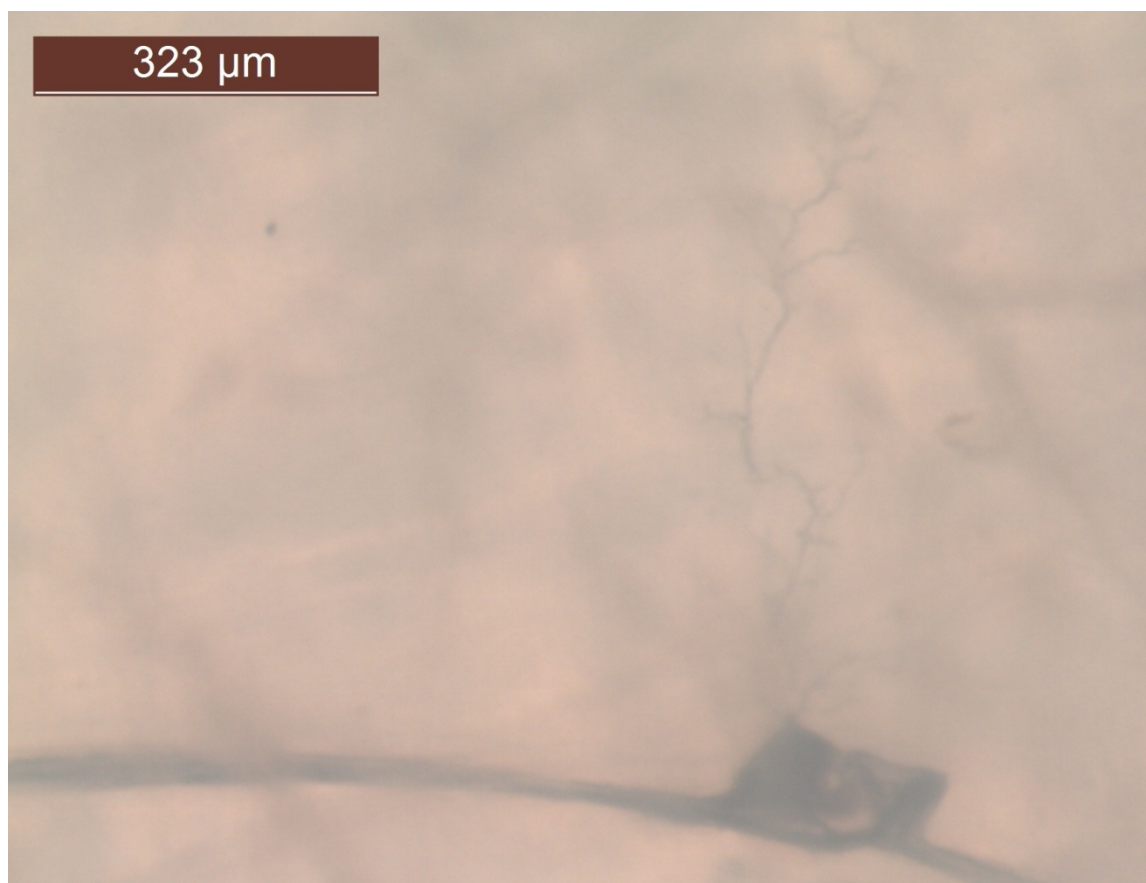


Figure 5.15 *Long tree of the branch type, initiated close to a kink. This test object was stressed by the positive voltage.*

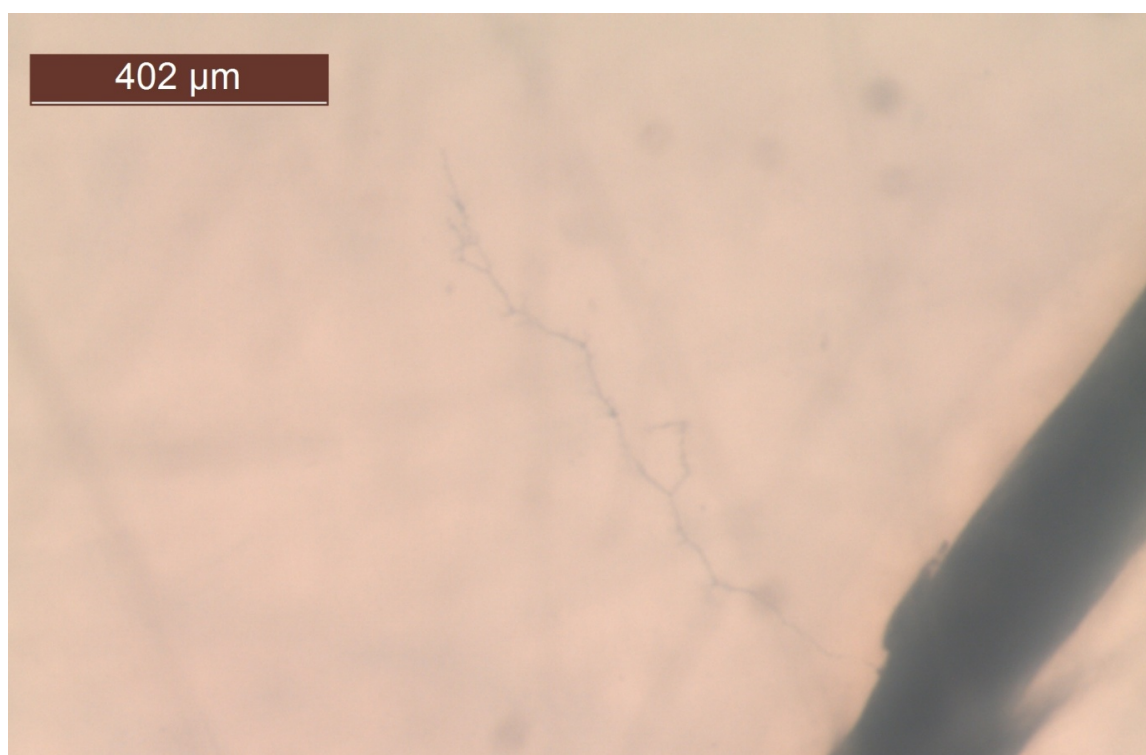


Figure 5.16 *Long tree of the branch type. This test object was stressed by the negative voltage.*



Figure 5.17 *Long tree of branch type, exhibiting the wider stem and stump like branches. This test object was stressed by negative voltage.*

The third case of electrical trees was observed close by the breakdown channel. This behaviour is also recognised for the slower voltage ramp rate analysed further on. In Figure 5.16 a comparatively large electrical tree has been formed by the breakdown channel.



Figure 5.16 *Test object showing both a breakdown channel and a smaller set of tree structured channels bridging the insulation.*

The last case of breakdown behaviour was present in three of the test objects, here only a small breakdown channel is formed and an example of this can be seen in Figure 5.17. An enlargement of this channel is shown in Figure 5.18, where it is clear that it has many branches and a tree like structure.

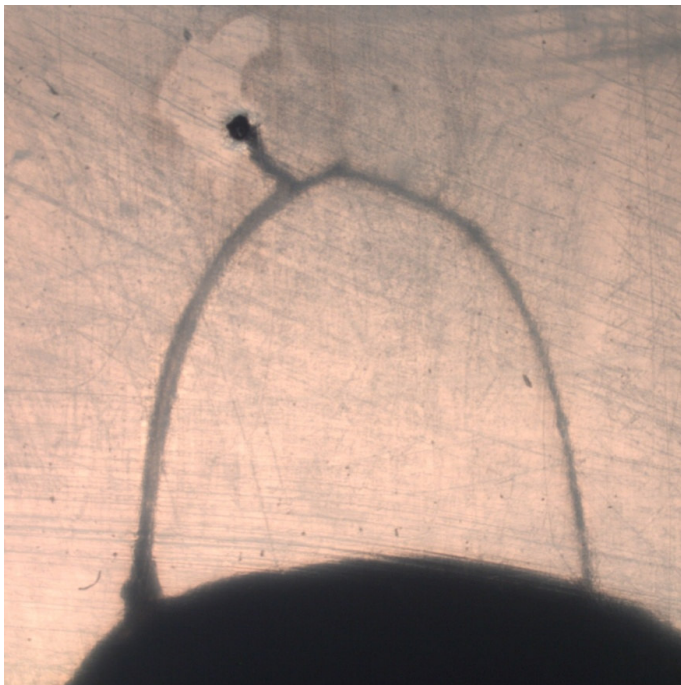


Figure 5.17 *Small breakdown channel.*

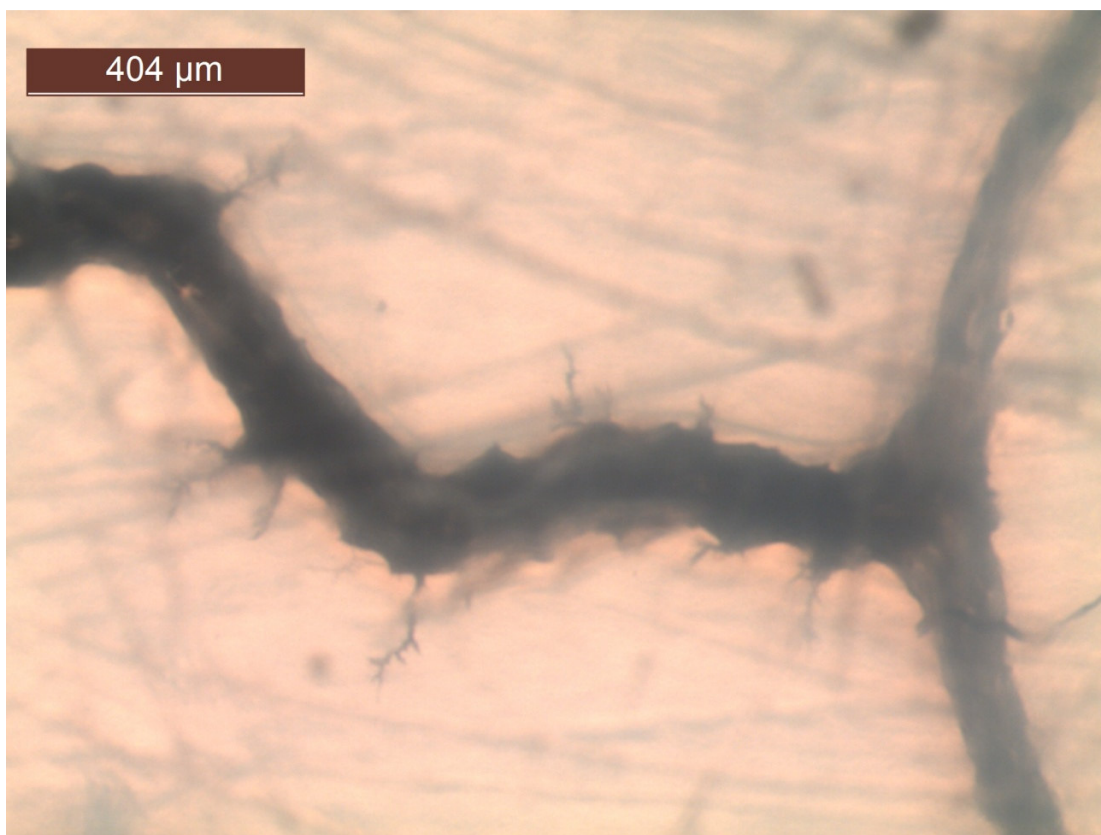


Figure 5.18 *A magnified image of the same channel as Picture 5.17. To the right in the picture the wire is seen.*

5.2.1.2 Weibull Analysis

The breakdown voltage has been compared between positive and negative polarity of the applied voltage. A two-parameter Weibull probability plot of the breakdown voltage is shown in Figure 5.19. As seen the breakdown voltage is significantly higher for negative than for positive polarity. A higher DC tree inception voltage for negative polarity has been found by [3] and [19].

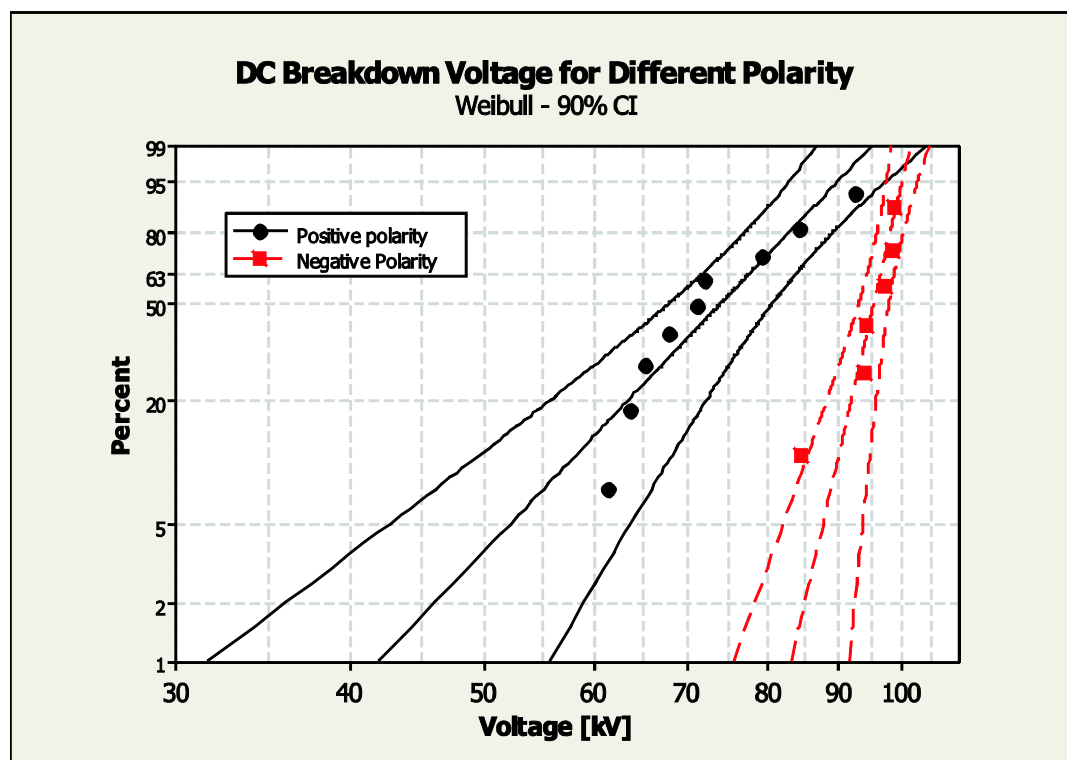


Figure 5.19 Two-parametric Weibull probability plot comparing the breakdown strength of the test object when stressed with negative and positive voltage at the faster ramp speed.

Negative polarity also had a higher shape and scale parameter. Negative polarity had a somewhat higher ramping speed than positive polarity. Ten samples were tested for each polarity; for positive polarity one of these had to be discarded whereas four samples were discarded for negative polarity. The Weibull parameters are collected in Table 5.6.

Table 5.6 Comparison of Weibull distribution parameters of DC breakdown voltage for positive and negative polarity.

Polarity	Ramping Speed	Shape, α	Scale, β [kV]	# samples
Positive	5.3 kV/s	7.5	77	9
Negative	-5.4 kV/s	31.0	96	6

5.2.2 Breakdown Tests at Ramping Speeds of ± 0.7 kV/s

To be able to do more comparisons with the AC results, efforts were made to try to get this method working for the lower voltage ramp speed as well. After many difficulties some progress, mostly for positive polarity of the applied voltage, was made and some results could be distinguished.

The aim was to use ten test objects of each polarity for this case as well, however this proved unachievable for the negative voltage and the tests at this polarity were aborted after three attempts, due to flashovers occurring repeatedly in the air between the high voltage conductor and ground. Some basics statistics is compiled in Table 5.7.

Table 5.7 *Sample statistics.*

Polarity	# samples tested	# samples with breakdown from the wire	# samples with tree structure detected
Positive	10	2	2
Negative	3	1	2

5.2.2.1 Breakdown Characteristics

Positive Polarity

For positive voltage polarity only two out of the ten test objects had breakdown originating from the surface of the wire. In five of the samples a breakdown channel was formed from the tab, probably from the end of the wire, see Figure 5.20. The remaining three test objects withstood the voltage for ten minutes after which the experiment was aborted.

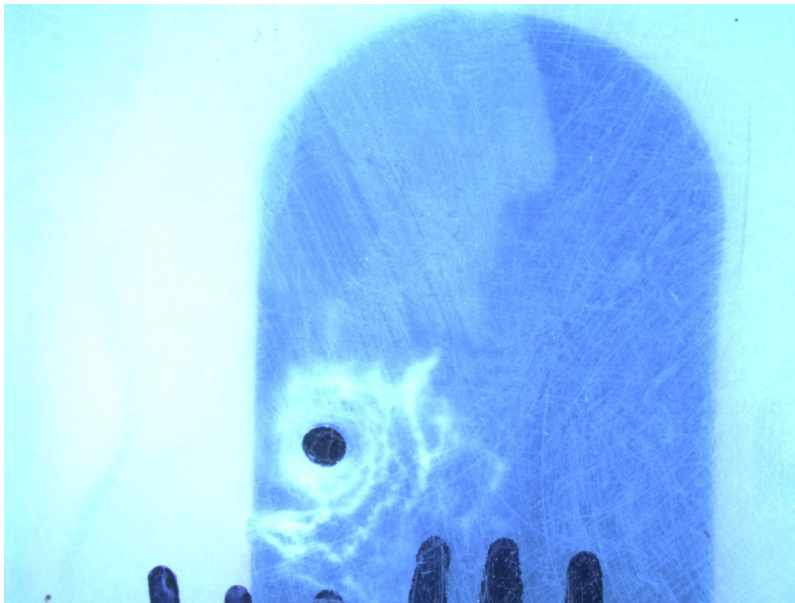


Figure 5.20 *Breakdown initiated at the semiconducting tab.*

Tree structure was only found on test objects which broke down at the wire. These long electrical trees of the branch type appeared close to the breakdown channel, examples are shown in Figure 5.21 and 5.22. For the test objects which broke down at the tab, no electrical trees have been detected.

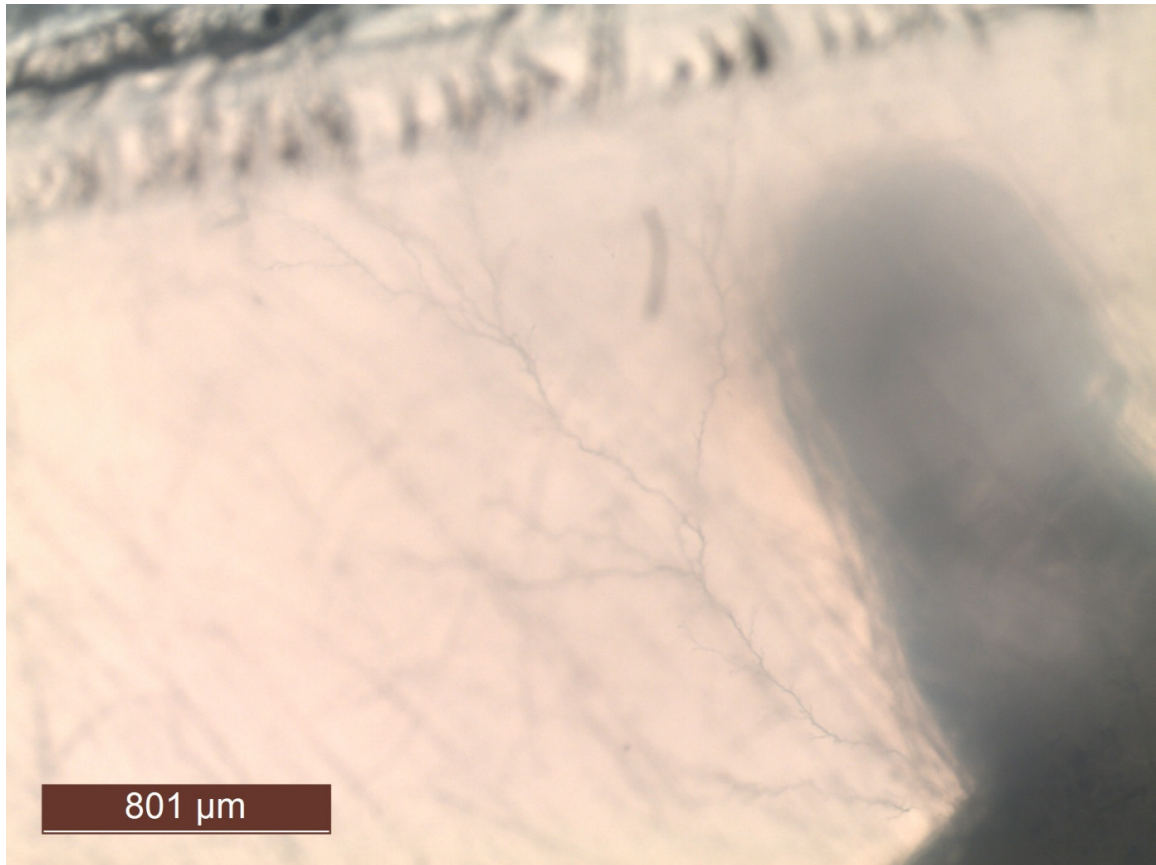


Figure 5.21 *Electrical tree of branch type at the breakdown channel.*

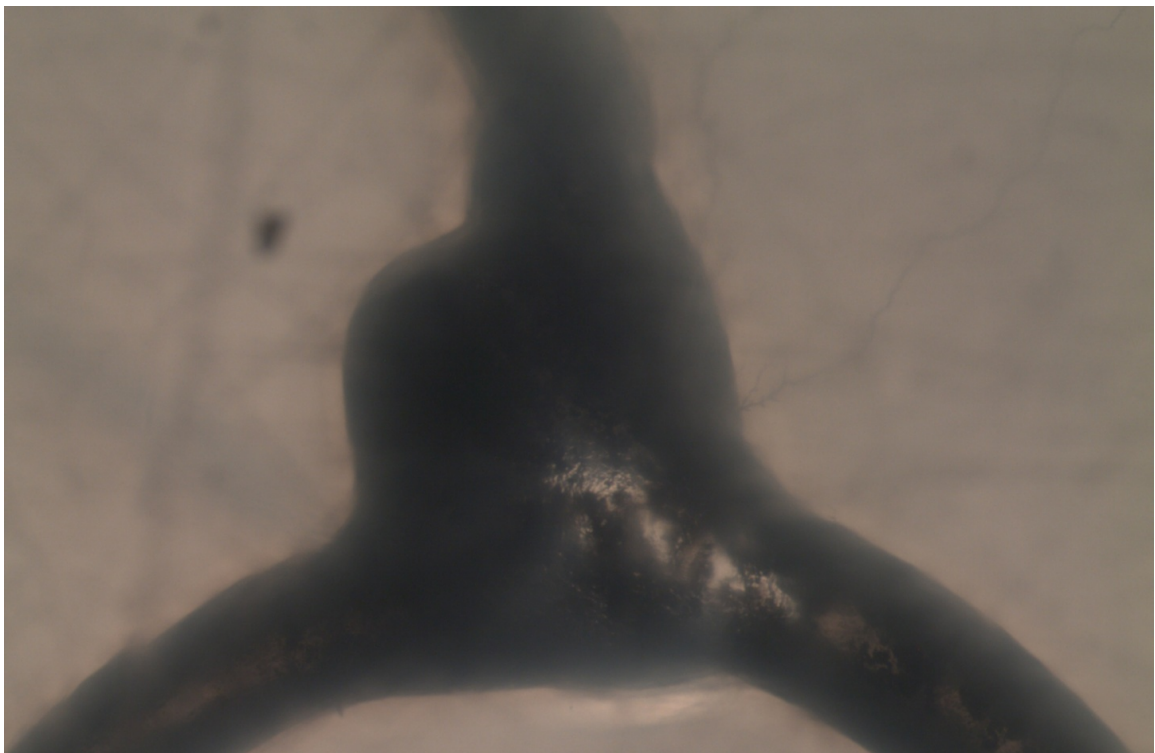


Figure 5.22 *Electrical trees at the breakdown channel.*

Negative Polarity

For negative polarity flashovers occurred between the high voltage conductor and the ground, before it was possible to recognise any trees on the video or there was breakdown in the test object. After trying 17 times altogether on three separate test objects, where only the first one broke down, the testing for negative polarity was aborted. Afterwards, when studying these test objects with the microscope several hundreds of tiny tree filaments were found along the wire, growing both towards the ground plane and towards the semiconducting tab. A portion of these tiny trees along a part of the wire can be seen in Figure 5.23.



Figure 5.23 Example showing tree filaments, found in abundance on the two abandoned test objects.

5.2.2.2 Weibull Analysis

Since only the positive polarity provided data on the breakdown voltage, this breakdown voltage is compared with the positive breakdown voltage at the lower ramping speed. A two-parametric Weibull plot, comparing the ramping speed of 0.7 kV/s with 5.3 kV/s, can be seen in Figure 5.24. It compares breakdown of the test object, but it should be considered that breakdown took place at the wire for the vast majority of the samples at 5.3 kV/s, whereas the breakdown took place at the semiconducting tab for the lower ramping speed. The breakdown voltage tends to be higher for 0.7 kV/s; this rate also has a lower shape and higher scale parameter. A comparison of DC tree inception voltage as a function of voltage ramping speed was made by [6], where it was found that the tree inception voltage decreases with increased voltage ramping speed. The Weibull parameters are collected in Table 5.8.

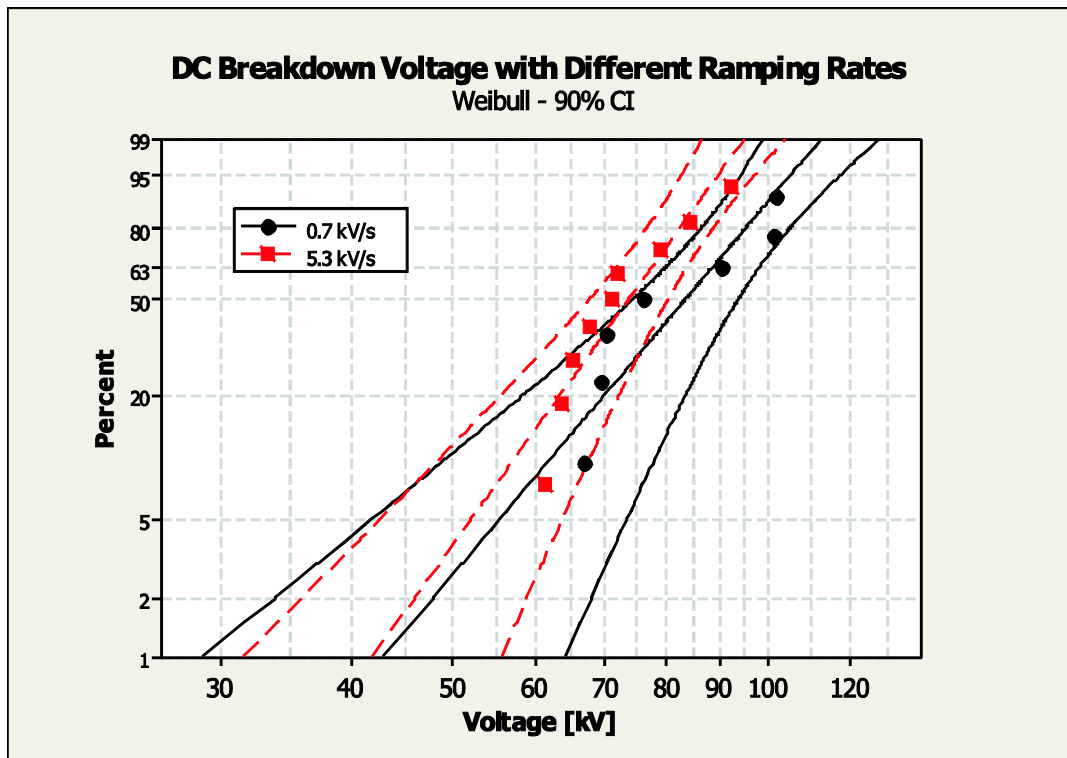


Figure 5.24 Two-parametric Weibull probability plot comparing the breakdown strength of the test object for the two ramping speeds at positive voltage polarity.

Table 5.8 Comparison of Weibull distribution parameters of positive DC breakdown voltage with respect to ramping speed.

Ramping Speed	Shape, α	Scale, β [kV]	# samples
0.7 kV/s	6.4	89	7
5.3 kV/s	7.5	77	9

5.2.3 Comparing the DC Results with the AC Results

Figure 5.25 illustrates the different kinds of trees found in the AC test objects; bush tree at a kink, mirror trees, mini-tree indicated by the arrow and bush-branch at the right most in the picture. These trees differ greatly in appearance from the trees observed in the DC stressed test objects, see Figure 5.26, which display a thin branch-like structure with very few branches. These thin trees have only been found in a couple of AC stressed test objects where a breakdown channel was formed. Worth noticing is also that when exposed to either DC or AC voltage the trees can grow both towards the ground plane and towards the semiconducting tab.



Figure 5.25 Several different varieties of trees found for AC voltage, the arrow is indicating a mini tree.

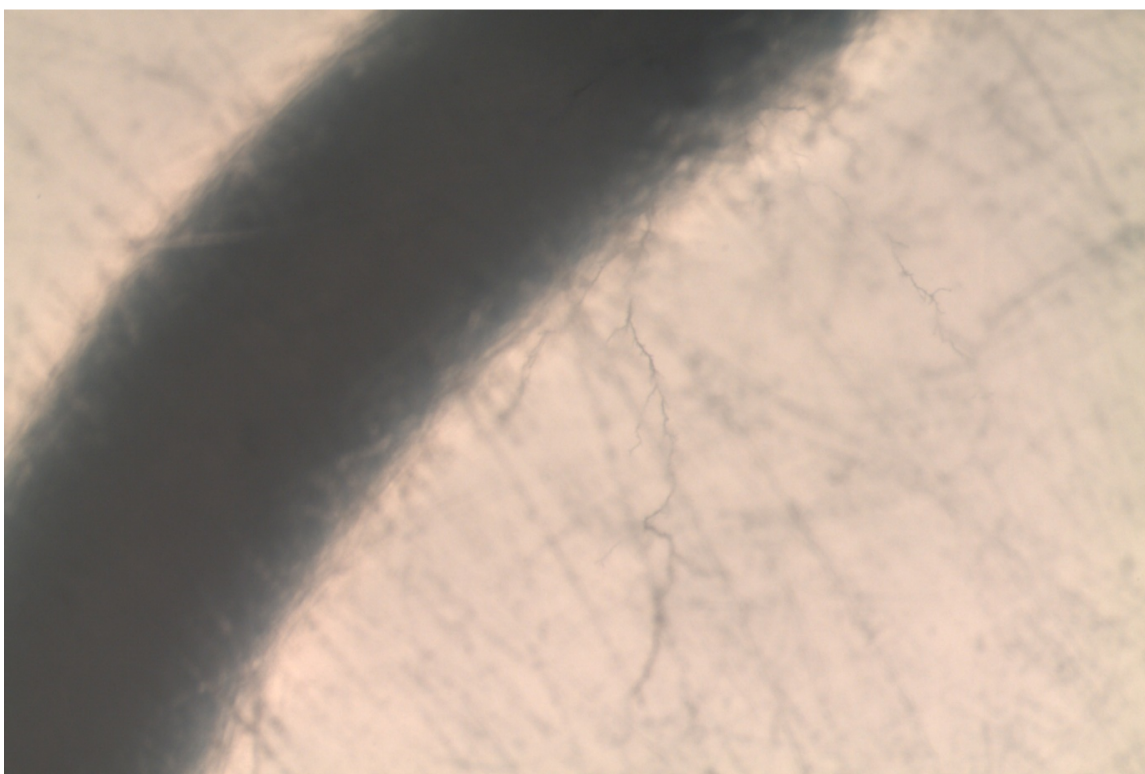


Figure 5.26 Branch trees or filaments found at the tube formed around the wire at a DC tested samples.

Furthermore, as can be seen in most of the DC images the XLPE has been changed around the breakdown channel and due to this the material has become more transparent and a distinct border between the two different material morphologies is clearly visible. This morphology change is only present in samples which have a breakdown channel, although it appears for both AC tests and for DC of both voltage polarities. In Figure 5.27 a tiny electrical tree can be seen growing from this interface.



Figure 5.27 A tiny tree growing from the interface between the two different material morphologies. The test object was stressed by the negative voltage.

Figure 5.28 shows the two-parametric Weibull distribution comparing AC treeing inception voltage and DC breakdown voltage of the higher ramping speed. It might be advisable to again point out that the same ramping function was used for this analysis but the rates differ since the DC voltage was lifted to the peak level whilst AC voltage is given as rms values. From the probability plot a distinct difference between AC and DC can be seen. Treeing inception occurs at a much lower voltage level for AC in comparison to the breakdown voltage of the DC stressed test objects, both polarities. Though keep in mind that two different processes are compared. It was done since it was not clear if the tree structures developed in the DC stressed test objects were initiated at the point of breakdown or were present before that. More studies need to be done to clarify when the filaments and tree structures are initiated in the XLPE exposed to DC voltage, see further discussion in Chapter 6.6.

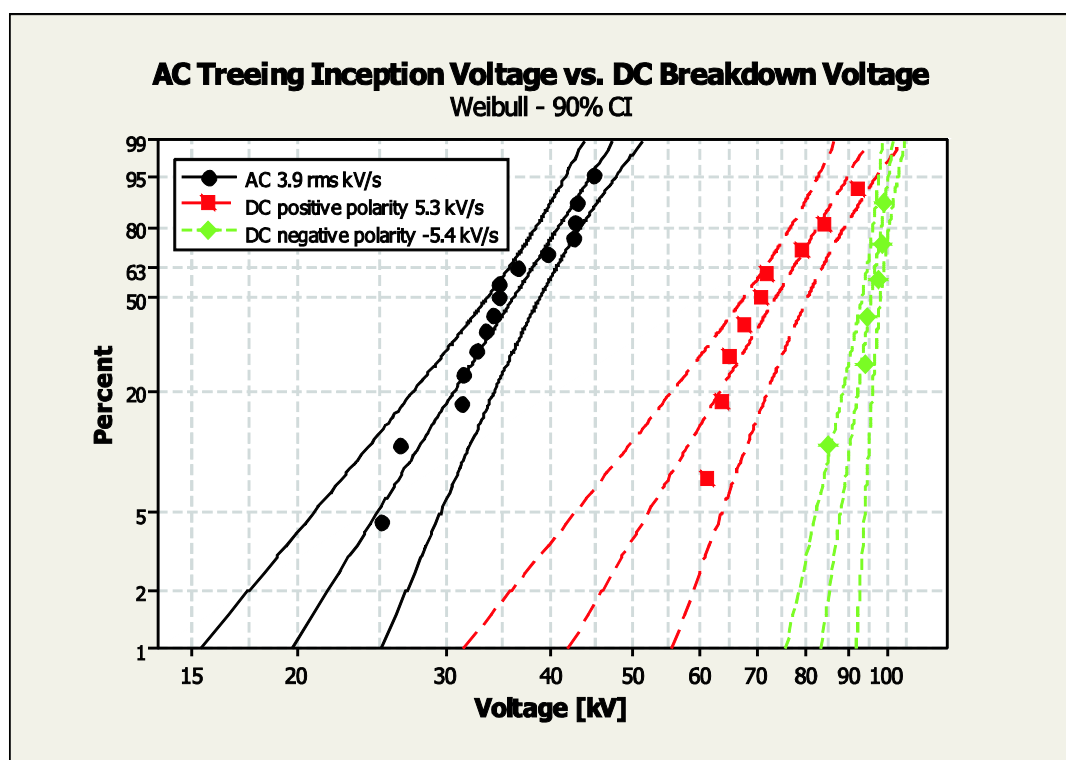


Figure 5.28 Two-parametric Weibull probability plot comparing AC treeing inception voltage with DC breakdown voltage for the ramping speed of 0.5 kV (rms).

The Weibull parameters are shown in Table 5.9. The shape parameters are high, negative polarity having a shape value of 31.0 though this is probably due to the low number of samples. The increase of amplitude of the scale parameter, AC being almost half the value of positive polarity and 40 percent of the negative polarity DC, reflects the trend already discussed.

Table 5.9 Comparison of Weibull distribution parameters of AC treeing inception voltage and DC breakdown voltage.

Voltage Type	Shape, α	Scale, β [kV]	# samples
AC, 3.9 kV/s	7.0	38	15
Positive DC, 5.3 kV/s	7.5	77	9
Negative DC, -5.4 kV/s	31.0	96	6

5.3 Temperature Impact on the Results

The temperature of the transformer oil was only measured for the DC experiments at 0.7 kV/s and for the AC test with a ramping rate of 3.9 kV/s, since a thermometer had not been acquired for the earlier conducted tests. The transformer oil became significantly heated by the lamp, the temperature varying between 23 °C and 41 °C. For every breakdown test made, where there was no need to replace the oil, this temperature would rise. By incident the test object subjected to the DC voltage broke down when the oil kept approximately the same temperature, only ranging between 25.7 °C and 26.9 °C, which ascertains that the results achieved in this test are not affected by the temperature but also that the impact of temperature on the DC tests cannot be concluded. For the 3.9 kV/s AC test, the tree initiation voltage has been plotted against the oil temperature, see Figure

5.29. These values look uncorrelated to the naked eye. A linear fit was made showing a slight dependence, though the correctness of this fit is questioned and it was assumed that the temperature difference of the oil did not affect the results obtained considerably. The temperature variation in the oil is however a source of error to take into account when considering the results. A study made by [28], where XLPE cable and needle-plane block samples were investigated for the temperature dependence of breakdown strength and tree inception voltage respectively, showed the same tendency of lower resistivity of treeing in the XLPE with higher temperature. This investigation was also made for AC voltage. This can be compared to Chapter 2.1.1.

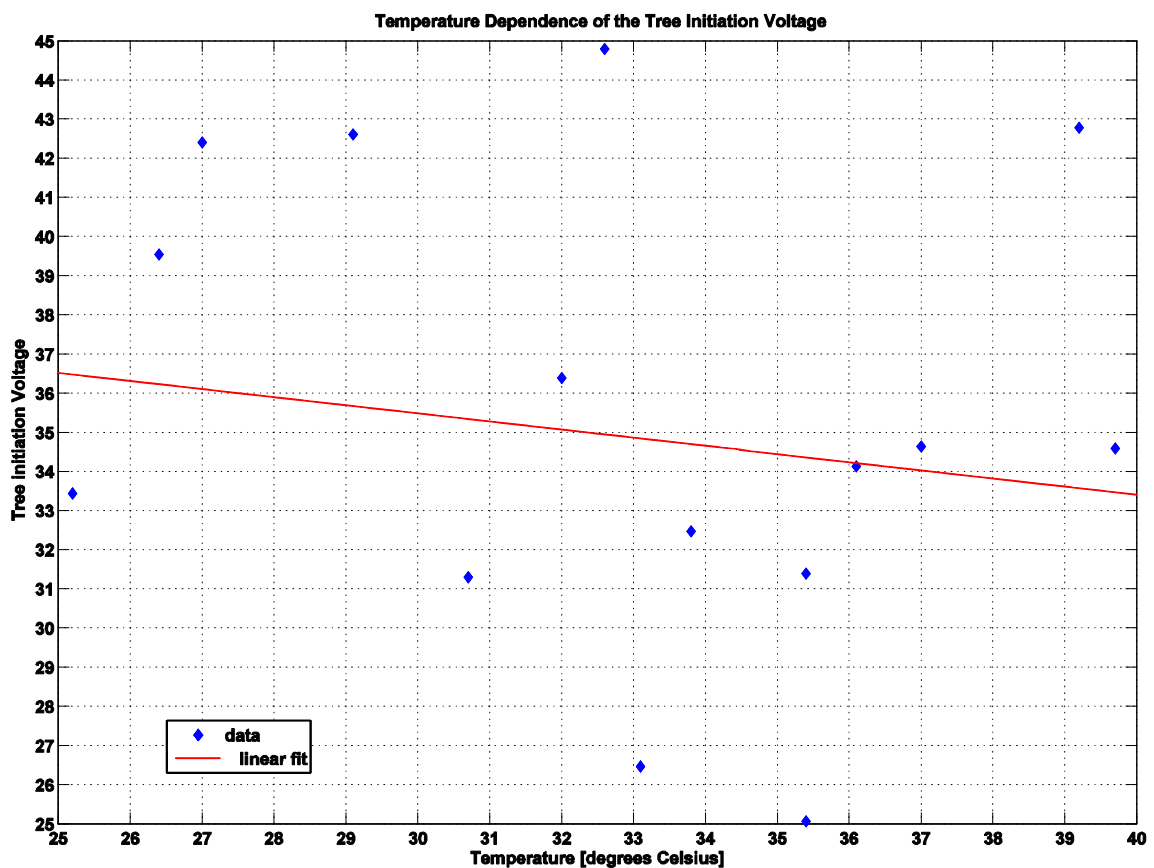


Figure 5.29 Correlation between temperature and tree initiation voltage for the AC test using the ramping speed of 3.9 kV/s.

6 Discussion

Relevant factors that could have influenced the experimental results will be discussed and some recommendations for future work are pronounced.

6.1 Kinks

Questions that arise regarding kinks are; why they appear and if tree inception voltage should refer to the first developed tree even though it appears at a kink and if kinks can affect treeing at the wire both close and far away. The analysis that follows are mostly based on the findings of the AC tested samples.

Kinks are created during the manufacture of test object, either by pressure in the pressing of materials or when the wire is sewn into the semiconducting tab. The latter seem to be more likely. The wire is very thin and was easily curled when touching a sharper point of the holes in the tab made for the wire to go through. The kinks cannot be seen by the eye and could therefore not been avoided without the use of a microscope. To what extent kinks would be present was not known in the beginning of the project so to use a microscope as a precaution was not done. A thicker wire might have helped to reduce the amount of kinks. A 20 μm wire was tested in the previous work and the problem with that configuration was that the voltage source available (the one used in this project) was not enough to initiate treeing for XLPE with added voltage stabilizers [7]. Since treeing with DC voltage requires much higher voltages than for AC treeing, which was the concern in the previous work, a thicker wire is not an option to avoid kinks. A thinner wire would be very difficult to handle manually when sewing it into the semiconducting tab and is probably not a solution either. The use of a microscope in the manufacturing process seems to be the simplest way to, if possible, reduce the amount of kinks present in test objects for future work.

Ought the tree inception voltage to be referred to the first tree at kink or at wire? Since every wire twist formation is unique it would not be possible to compare the local electric field around them without very thorough analysis. The inception voltages for trees developed at kinks are therefore not relevant for electric treeing studies of a certain electrode configuration, not said that there is no trend in inception voltages for treeing at kinks, see Figure 5.6. Trees are initiated at lower voltage levels when grown at kinks than originating from the wire. The range of stress levels are wider for treeing at kinks which probably is due to variations of kink geometries, some being sharper than others resulting in more divergent electrical fields which will affect the tree inception voltage. The wire being conformable with the same divergent field all around is on the other hand easily modelled to make a relation between inception voltage and initiation field, which was done by Huuva [7]. It made the comparison in Chapter 5.1.2 possible. It would also make it easier to compare with other electrode configurations though it was not done in this project.

Then it comes to the question whether the kinks can affect treeing at other places along the wire, both in the vicinity and further away. First, it needs to be stated that there were relevant data to make an analysis. The amount of samples used for the analysis is only enough to speculate a theory not to make any clear statements which one should have in mind when reading the following discussion. From Table 5.4 the mean number of kinks per sample can be calculated to 1.4 and 1.5 for the lower and higher rate respectively which means that the percentages are comparable. If one rate would have had the majority of the wire defects no conclusions could be made. It was seen that the fraction of kinks with and without trees were very similar for the both ramping rates. The only thing that differed distinctly was whether the first inception tree arises from a wire defect or not; 12 out of 19 (63%) for the lower rate and 2 out of 10 (20%) for the higher rate. It seems that the tree inception voltages for the lower rate were more dependent on electrode geometry than for the higher rate. The low fraction of trees actually originating from a kink for the higher ramping rate is an indication that the kinks will not influence the inception of electrical trees at the wire, for this speed. The electrical treeing seems instead to be connected to other physical processes; further discussion will follow in Chapter 6.5.

Second, how would it be possible for a wire defect to influence treeing? One thing might be the alteration of morphology and thereby density around the defect. Another might somehow be connected to the first tree to appear at a kink and to the partial discharges and energy release associated with tree formation. Both suggestions are connected to phenomena that are likely to influence only the close vicinity of kinks and no trend of more trees around them could be seen. Most are developed at the tip of the kink only. Thereby also the results for the lower ramping rate are thought not to be influenced by the presence of kinks.

6.2 Visual Limitations and Requirements

The study of electrical trees with optical detection has its requirements and limitations. The wire must be of a size that can be detected with the camera and it should be controlled to be close to the tab for the ability to see both wire and grounding plane in the same frame. The latter will enable measurements of tree growth rate. For every new specimen observed in this work, as much of the wire as possible had to be placed in the frame.

To avoid flashovers in the surrounding circuit transformer oil served as insulation around the test object. If clean this oil is very transparent and well suited for optical detection. It is though inevitable to have small particles present since the experiments are not carried out in a “clean room”. These small particles can be fibres from paper used to wipe the aquarium and small threads from clothing that is hard to detect visually but can be seen in pictures taken by the CCD camera. In turn, the filaments developed with DC voltage stress could not be observed by the camera, for this the microscope was needed.

The biggest obstacle for optical detection was encountered when there was a breakdown as for most of the DC tests. Since the semiconducting tab melted and coloured the oil this reduced the optical detection abilities severely. If not too coloured the oil was filtered, as described in Chapter 4.3. If this was not enough the transformer oil had to be exchanged to new oil. This becomes both costly and time consuming. It should also be considered that the properties of the transformer oil might be altered.

In this project the initiation of treeing was determined by the study of picture frames; that there was a change from one frame to the next. With the camera used it was impossible to detect the distance of $\sim 5 \mu\text{m}$ of tree growth which is a defined length for a tree to be initiated [10]. An exact determination of initiation voltage might need electrical measurements such as dielectric response measurements. Electro luminescence, which is another electrical treeing detection method, cannot be used for DC voltage [9]. To standardize the definition of change by either a certain amount of pixels or a specified length, as in [29], might be a solution. The last one though will have a problem with tree development at different speeds and the accuracy can be questioned for this method. With a short tree length it will be the same as defining a number of pixels. With an amount of pixels enough to without doubt confirm a change due to electrical treeing will be the recommendation for future work.

From the microscopic study of the test objects no voids with a size $\geq 2 \mu\text{m}$ could be found. Smaller might not have been possible to detect with certainty. The formation of voids is a problem when using needle electrode since the tree inception field will depend upon the void size [9]. The wire-plane configuration seems to have overcome this disadvantage.

6.3 Silver Flakes

The removal of silver paint is thought not to influence the treeing process. Since the pair of tweezers was pressing the test object towards the grounded copper bar good connection was secured also without the paint. The flakes with floating potential are not likely to make any significant change to the local electric field strength due to a larger distance from the high potential electrode than the grounding plane if not located at the absolute vicinity of the sample surface, which was only the case once. Also, regarding tree growth, especially bush tree propagation, the space charge distribution is considered to have a higher effect on the local electric field than the electrode geometry once a tree is initiated [9], a silver flake could be considered a part of the electrode arrangement in this case.

6.4 Accuracy of Voltage Measurements

Manual regulation will lead to errors. The assumption to start LabView exactly ten seconds after the camera was evaluated to have a maximum time error of 0.7 seconds and a mean error of 0.4 seconds, see Chapter 4.4.1. For AC treeing inception voltage determination this error will affect Δt in Formula 4.1, i.e. the time it takes for the first tree to initiate counted from the ramp start and as a consequence the voltage levels presented could be too low. For the ramping speed of 0.53 kV/s ($\approx 0.5 \text{ kV/s}$) and 3.86 kV/s ($\approx 3.9 \text{ kV/s}$) it corresponds to a maximum deviation of 0.4 kV and 2.7 kV respectively. This means that it might be a bigger difference for AC initiation fields with different ramping speeds, making the separation of the two Weibull distributions more distinct. In the comparison with the previous work [7] the lower ramping rate could in the worst case have a 7.2 kV/mm too low initiation field, though the values are still in range with the earlier results and will be further discussed in 6.5 AC Phenomena. The voltage levels for the kink analysis are connected to the same amplitude of error due to the same ramping rate, the comparison is thereby unaffected. For the DC voltage determination this time error

omitted since it can be clearly seen in the voltage measurement at which voltage level the breakdown took place.

The assumption that the AC voltage signal was symmetric around the offset value was justified since the mean error was estimated to -0.05 kV for the slower speed and -0.03 kV for the faster speed, the minus sign indicating the presented voltage levels in results to be too low, though the difference is negligible. This asymmetric AC voltage is considered the source of the differing ramping speeds of the two voltage polarities in DC.

The last assumption made for AC voltage determination regarding the sampling frequency which resulted in peak loss of the sinus wave for some periods was reduced by using linear fitting function and the maximum deviation from a peak was estimated to 0.45 kV. The sampling frequency will also affect the DC voltage measurements in an analogous way and this will be the largest error introduced in these measurements.

The accuracy of the DAQ introduces the smallest of the errors involved with a maximum of ± 3.6 V as discussed in Chapter 4.2.1.

6.5 AC Phenomena

In the comparison with the previous work [7] it could be concluded that the obtained results were in the same range as for the previous work. The values thereby gain validity and the test configuration is proven to be repeatable. The difference of distribution parameters is probably coupled with both quantity of tested samples and that the XLPEs were not exactly the same regarding morphology and added stabilizers.

In the comparison of AC treeing initiation fields with different ramping rates it was seen that the higher speed was also the one with the higher initiation field. For DC voltages, both polarities, it has been proven to be the other way around [29]. At first sight this seems to be the logic trend also for AC voltage tests since the dielectric is stressed with a higher voltage amplitude. Since this is not the case a time constant must be involved. It takes a certain time for charge injection to build a net space charge enabling the first breakdown. With a faster voltage rise a higher level is reached when the first tree appears. It should be noted in this context that only one breakdown channel appeared for the lower ramping speed while it was six channels for the faster speed. The difference might be due to a larger stress once treeing is initiated. Though, a more likely cause is connected to the fact that the applied voltage was kept a bit longer for the tests made with higher ramping rate than the low ramping rate. The voltage source was manually turned off when the electrical trees covered approximately half the distance to the grounding plane. The higher ramping rate was the last test made and the consequences of a breakdown were known not to destroy any equipment so the voltage was applied a bit longer with the attention to make more developed tree-structures possible. The tree growth rate was also faster for the higher ramping rate which was illustrated by Figure 5.4 and 5.5 and it was therefore more difficult to turn off the applied voltage in time before the XLPE breakdown. Altogether it resulted in the little extra time needed for breakdown channel to arise and increasing this statistics for the higher ramping rate.

6.6 DC Phenomena

The half-wave rectifier was adequate in supplying a smooth DC voltage. As was shown in the results the ripple was less than 0.6 % of the applied voltage. Since only a small current was drawn by the circuit the capacitors could lift the voltage to approximately the peak value of the AC voltage supplied by the transformer. Due to this the ramping speed was a square root of two times higher for the DC voltage. The time constants of the resistors and the capacitors will also affect the ramping speed, but this influence was found to be negligible.

Some complications were encountered when attempting to observe the trees in real time with the camera. One reason for this could be that the treeing process happened too fast for the camera to observe it. From not being able to distinguish any electrical trees in one picture frame, a complete breakdown of the test object had occurred in the following. Another reason could be that trees were present in the XLPE for some time, but that they were too thin or light to be discerned. The samples which broke down at the tab provided no images of the breakdown at all, since the breakdown happened outside the frame. In the future, when manufacturing test object the thickness of the insulation covering the semiconducting tab should be considered and perhaps increased to prevent breakdown channels originating from the tab. These channels might also stem from the cut ends of the wire placed at the tab, so some adaption might be needed on the design of the test objects.

During the DC experiments a considerable percentage of the test objects had to be discarded since the maximum voltage was not enough for some samples to either initiate treeing or breakdown, or since the voltage would cause a flashover at a different location in the test setup. A voltage source with a higher maximum might initiate treeing but would probably introduce several new complications. Another solution, using the same voltage source, would be to change the test procedure; prestressing the test objects with AC voltage or perform grounded and constant DC tests. The flashover was most likely to take place at the oil surface between the high voltage conductor and the ground wire, which connected the copper bar with common ground. In order to reduce the risk of this a larger aquarium would be necessary.

For the DC experiments it is uncertain whether the electrical trees were initiated during the ramping of the voltage, during the sharp voltage drop at breakdown or during the following oscillations. All these options are possible causes of tree initiation and breakdown in the test object. It is also dubious if the breakdown channels formed started as electrical trees or if there are other processes involved. A supposition is that the thicker trees with stump like branches were present before the breakdown channel appeared, since it seems as if the breakdown current have affected them. Whereas the extremely thin trees appearing at the breakdown channel or at the widened tube around the wire might either be formed during the voltage drop or the oscillations, though it is uncertain which of these processes would have initiated them. The thin trees were also discovered in a couple of AC stressed test objects which experienced complete breakdown; this would make it plausible that the steep voltage drop initiated them and that they grew rapidly. The remaining voltage, following the breakdown and the oscillations, complicates the matter further as the level is too high to be disregarded. The mainly long trees, found in the test

objects stressed with DC voltage, tend to be of the branch type, this is especially illusory when compared to the more bushy AC trees. This tendency was also found in [30] where the electrical trees initiated and grown at a 50 Hz voltage stress were bush like, whereas for decreasing frequency of the applied voltage they became longer and had fewer branches.

Regarding the tiny trees found at the negative polarity even more parameters have to be considered as these test objects were stressed repeatedly. This was done as the voltage caused a flashover elsewhere in the circuit numerous times.

7 Conclusions

The newly developed test configuration for detection of electrical treeing with a wire-plane electrode geometry is possible to reproduce and can be performed with both DC and 50 Hz AC voltage applied. The DC voltage was in this project achieved from an AC source using a half-wave rectifier and capacitors to smooth the ripple.

Electrical treeing in XLPE insulation due to DC stress requires high voltages, probably in the range of 60 kV to 100 kV. The main problem in building an experimental setup for these voltages was flashovers in the surrounding circuit. It is concluded that a ramping speed of 5.5 kV/s makes tests possible for both DC voltage polarities.

Electrical tree structures in the test objects stressed with a DC voltage could not be distinguished by the CCD camera before a complete breakdown of the XLPE occurred. With microscopic observations carried out after the experiments, filaments and branch trees were found. The inception voltage levels for these tree structures were not known and therefore the DC breakdown voltages were compared with treeing inception voltages caused by AC stress. The purpose of determining the treeing initiation field was not possible for the DC tested material. The required voltage levels for both polarities of DC breakdowns were significantly higher than the AC treeing inception voltage. For DC voltage it is also apparent that the breakdown voltage is lower for positive polarity than for negative polarity.

In AC tests the higher ramping rate of 3.9 kV/s (rms) resulted in a higher treeing initiation field than for the lower rate of 0.5 kV/s (rms). For the DC voltage of positive polarity breakdown voltages were compared for the two ramping rates. In this case it is concluded, the dielectric material withstood a higher voltage for the slower speed.

The filaments and branch-trees discovered in the test objects exposed to DC voltage are similar in shape to the ones observed in an AC stressed sample which developed a breakdown. Also bush, bush-branch, mirror-trees and mini-trees could be identified for AC stressed specimens.

8 Future Work

The main focus for further studies should be trying to measure the electrical treeing initiation voltage for DC. In order to manage this, optical detection with a higher resolution is required since it was not possible to distinguish electrical trees.

Additional DC test methods could be investigated, such as grounded and constant DC. Other ramping speeds or an even higher voltage level might also be used. For this, attention to the surrounding circuit is needed to avoid flashovers.

Some modifications of the test specimens are recommended. For further work the samples could be thicker to avoid breakdowns through the width of the test objects. The wire should be sewn with a loop close to the tab, so that the camera captures both the whole wire and the grounding plane. This enables analysis of the tree growth rate. A microscope should also be included as a part of the optical detection to enable discovering filaments and mini-trees. For a more thorough investigation of the trees and breakdown channels it is suggested to slice the test objects. Moreover, this enables detection of morphology changes of the XLPE, especially along the wire and at the possible border where the two stripes are cross-linked together.

The temperature of the transformer oil was raised several degrees Celsius for some tests due to the available light bulb. The risk of errors due to heated oil can probably be reduced by utilizing a lighting source made for photographic use.

Finally, it would be interesting to use an automatic control of voltage regulation and measurement for reduction of the errors connected to manual regulation. This could be combined with electrical detection of electrical treeing.

References

- [1] G. Chen, C. H. Tham. “Electrical Treeing Characteristics in XLPE Power Cable Insulation in Frequency Range between 20 and 500 Hz”, *IEEE Transactions on Dielectrics and Electrical Insulation*, Vol. 16, pp. 179-188, 2009
- [2] X. Zheng and G. Chen, “Propagation Mechanism of Electrical Tree in XLPE Cable Insulation by investigating a Double Electrical Tree Structure”, *IEEE Transactions on Dielectrics and Electrical Insulation*, Vol. 15, pp. 800-807, 2008.
- [3] H. Kawamura and M. Nawata, “dc Electrical Treeing Phenomena and Space Charge”, *IEEE Transactions on Dielectrics and Electrical Insulation*, Vol. 15, pp. 741-747, 1998.
- [4] M. Selsjord, E. Ildstad, “Electrical Treeing Caused by Rapid DC-Voltage Grounding of XLPE Cable Insulation”, Conference Record of the 2006 IEEE International Symposium on Electrical Insulation, 11-14 of June, 2006, Toronto, Canada.
- [5] J. Liu, Q. Zhou, D. Ye, T. Yang, R. Liao, S. Chen, “Study on Propagation Characteristics of Electrical Trees in different Electrode System”, 2008 International Conference on High Voltage Engineering and Application, 9-13 of November, 2008, Chongqing, China.
- [6] M. Ieda and M. Nawata, “DC Treeing Breakdown Associated with Space Charge Formation in Polyethylene”, *IEEE Transactions on Electrical Insulation*, Vol. EI-12, pp. 19-25, 1977.
- [7] R. Huuva. “New Test Arrangement for Measuring Electrical Treeing Resistance in Polymers”, Thesis for the Degree of Licentiate of Engineering, Department of Materials and Manufacturing Technology, Chalmers University of Technology, 2007
- [8] ASTM D 3756 – 97, Standard Test Method for Evaluation of Resistance to Electrical Breakdown by Treeing in Solid Dielectric Materials Using Diverging Fields, 2001.
- [9] L. A. Dissado and J.C. Fothergill, “Electrical Degradation and Breakdown in Polymers”, IEE Materials and Devices Series 9, Peter Peregrinus Ltd., London, the United Kingdom, 1992.
- [10] L. A. Dissado, “Understanding Electrical Trees in Solids: From Experiment to Theory”, *IEEE Transactions on Dielectrics and Electrical Insulation*, Vol. 9, pp. 483-497, 2002.
- [11] K. Wu and L. A. Dissado, “Model for Electrical Tree initiation in Epoxy Resin”, *IEEE Transactions on Dielectrics and Electrical Insulation*, Vol. 12, pp. 655-668, 2005.

- [12] V. Englund, R. Huuva, S. M. Gubanski and T. Hjertberg, "Synthesis and Efficiency of Voltage Stabilizers for XLPE Cable Insulation", *IEEE Transactions on Dielectrics and Electrical Insulation*, Vol. 16, pp. 1455-1461, 2009.
- [13] A. Xie, S. Li, X. Zheng and G. Chen, "The characteristics of electrical trees in the inner and outer layers of different voltage rating XLPE cable insulation", *Journal of Physics D: Applied Physics*, Vol. 42, 125106, 2009.
- [14] B. R. Varlow and D. W. Auckland, "The Influence of Mechanical Factors on Electrical Treeing", *IEEE Transaction on Dielectrics and Electrical Insulation*, Vol. 5, pp. 761-766, 1998.
- [15] R. J. Densley, "An Investigation into the Growth of Electrical Trees in XLPE Cable Insulation", *IEEE Transaction on Electrical Insulation*, Vol. EI-14, pp. 148-158, 1979.
- [16] A. S. Vaughan, I. L. Hosier, S. J. Dodd and S. J. Sutton, "On the structure and chemistry of electrical trees in polyethylene", *Journal of Physics D: Applied Physics*, Vol. 39, pp. 962-978, 2006.
- [17] C. Laurent and C. Mayoux, "Analysis of the propagation of electrical treeing using optical and electrical methods", *IEEE Transactions on Electrical Insulation*, Vol. EI-15, pp. 33-42, 1980.
- [18] J. C. Fothergill, L. A. Dissado and P. J. J. Sweeney, "A Discharge-Avalanche Theory for the Propagation of Electrical Trees", *IEEE Transactions on Dielectrics and Electrical Insulation*, Vol. 1, pp. 474-486, 1994.
- [19] Y. Sekii, H. Kawanami, M. Saito, K. Sugi and I. Komatsu, "DC Tree and Grounded DC Tree in XLPE", Annual Report of the IEEE Conference on Electrical Insulation and Dielectric Phenomena (CEIDP), pp. 523-526, 16-19 of October, 2005, Nashville, Tennessee, the USA.
- [20] R. Huuva, V. Englund, S. M. Gubanski, T. Hjertberg. "Development of New Test Setup for Investigation of Electrical Tree Inception in Polyethylene", Proceeding of the 19th Nordic Insulation Symposium, pp. 178-181, 13-15 of June, 2005, Trondheim, Norway.
- [21] "Comsol Multiphysics", Comsol AB, Sweden, 2006.
- [22] R. Ross, "Bias and Standard Deviation due to Weibull Parameter Estimation for Small Data Sets", *IEEE Transactions on Dielectrics and Electrical Insulation*, Vol. 3, pp. 28-42, 1996.
- [23] IEEE Standard 930-2004, "Guide for the statistical analysis of electrical insulation breakdown data", 2007.

- [24] D. Cousineau, "Fitting the Three-Parameter Weibull Distribution: Review and Evaluation of Existing and New Methods", *IEEE Transactions on Dielectrics and Electrical Insulation*, Vol. 16, pp. 281-288, 2009.
- [25] G. C. Montanari, G. Mazzanti, M. Cacciari, J. C. Fothergill, "In Search of Convenient Techniques for Reducing Bias in the Estimation of Weibull Parameters for Uncensored Tests", *IEEE Transactions on Dielectrics and Electrical Insulation*, Vol. 4, pp. 306-313, 1997.
- [26] T. Andrews, R. N. Hampton, A. Smedberg, D. Wald, V. Waschke and W. Weissenberg, "The Role of Degassing in XLPE Power Cable Manufacture", *IEEE Electrical Insulation Magazine*, Vol. 22, pp. 5-16, 2006.
- [27] R. Huuva, V. Englund, S. M. Gubanski, T. Hjertberg. "A Versatile Method to Study Electrical Treeing in Polymeric Materials. *IEEE Transactions on Dielectrics and Electrical Insulation*, Vol. 16, pp. 171-178, 2009
- [28] A. Ishibashi, T. Kawai, S. Nakagawa, H. Muto, S. Katakai, K. Hirotsu, T. Nakatsuka, "A Study of Treeing Phenomena in the Development of Insulation for 500 kV XLPE Cables", *IEEE Transactions on Dielectrics and Electrical Insulation*, Vol. 5, pp. 695-706, 1998.
- [29] M. Ieda, "Dielectric Breakdown Process of Polymers", *IEEE Transactions on Electrical Insulation*, Vol. EI-15, pp. 206-224, 1980.
- [30] F. Mauseth, E. Ildstad, M. Ytterstad, R. Hegerberg, B. Sanden, M. Jeroense, J. E. Skog, "Quality Control of HVDC Extruded Cables: Electrical Treeing in XLPE under Different Voltage Stresses" Proceedings of the 16th International Symposium on High Voltage Engineering, ISBN 978-0-620-44584-9, 24-28 of August, 2009, Cape Town, South Africa.

